CHALMERS

Characterization of Emissions from Hybrid and Plug-in Hybrid Medium-Duty Electric Vehicles

Aryan Dawody

4/4/2014

Abstract

Measured data obtained from rig tests, on-road hybrid, plug-in hybrid and conventional diesel powertrains and buses have been analyzed to evaluate the emissions and fuel consumption under different driving cycles. Major attention has been given to the performance of the exhaust aftertreatment system (EATS) with respect to emission (i.e., NO_X, PM, THC and CO) conversion under the tested conditions with the purpose of identifying the conditions under which the emissions targets are not meet and evaluate the source of the largest obstacles.

The on-road tests consisted of testing two hybrid buses and one conventional diesel bus during summer and winter time. The test cycles included urban, sub-urban and mixed driving conditions in addition to a plug-in hybrid bus which was tested on the bus 60 route cycle in Gothenburg. The rig tests consisted of testing regular hybrid and plug-in hybrid with and without heat modes in an engine bench using two different test cycles. The heat modes used in the rig test series tests were used to increase the exhaust temperature by oxidation of controlled amounts of diesel to the diesel oxidation catalyst in the EATS system. All vehicles used in the on-road tests were equipped with Euro V EATS systems, while the rig test systems were equipped with Euro VI EATS systems.

The analysis shows that the exhaust temperature upstream the selective NO_X reduction catalyst (SCR) and the availability and amount of the NO_X reducing agent, urea, are two crucial parameters for NO_X conversion. From the on-road tests the conventional diesel bus reached the lowest levels of specific NO_X emissions. A large variation was observed in SCR-catalyst performance during the rig tests of plug-in and regular hybrid setups, depending on what cycle was tested and the engine power output. The cycle run that had the lowest specific tailpipe NO_X was one of the plug-in hybrid tests performed on the City 2 cycle, which in comparison to the other tests had the highest energy output, a high mean exhaust temperature upstream the SCR unit and the highest urea/NO_X ratio. The analysis of the temperature profiles shows that the heat modes implemented in the plug-in hybrid tests were able to increase the exhaust temperature although not to the levels which are required for optimal NO_X conversion. The analysis also shows evidence for high NH_3 storage capacity in the SCR catalyst since NO_X conversion was observed at conditions when no urea injection is on-going.

Keywords: Hybrid, Plug-in hybrid, emissions, exhaust aftertreatment, NO_X, fuel consumption

Contents

Acknowledgments

This master thesis was conducted at Energy Efficiency and Environment (EEE), Advanced Technology and Research (AT&R) Volvo Group Trucks Technology (GTT).

I would like to offer my gratitude towards Dr. Behrooz Razaznejad, Director of Exhaust Aftertreatment Systems (EATS), for giving me the opportunity to do my thesis in his group.

I am truly thankful to Prof. Bengt Andersson my examiner and supervisor at Chalmers, for his valuable input to my thesis.

I would also like to give great thanks to my supervisor at Volvo Dr. Jan Koegler for his support throughout my work.

Many thanks to the people in the EATS group at EEE/AT&R, in particular to Dr. Lennart Andersson, Dr. Miroslawa Milh, Dr. Martin Lundén and Dr. Jazaer Dawody for supporting me when needed.

Last but certainly not least I would like to thank my wonderful family and friends for their love and support.

Abbreviations

AHI	**Aftertreatment Hydrocarbon Injector**
ASC	**Ammonia Slip Catalyst**
DOC	**Diesel Oxidation Catalyst**
DPF	**Diesel Particulate Filter**
EATS	**Exhaust Aftertreatment System**
EGR	**Exhaust Gas Recirculation**
FTIR	**Fourier Transform Infrared**
HDV	**Heavy Duty Vehicle**
HEV	**Hybrid Electric Vehicle**
ICE	**Internal Combustion Engine**
PHEV	**Plug-in Hybrid Electric Vehicle**
PM	**Particulate Matter**
PN	**Particulate Number**
SCR	**Selective Catalytic Reduction**

1. Introduction

1.1 Background

Concerns emerged from limited availability of fossil fuel and the deteriorated air quality due to emissions from fossil fuel combustion have driven the automobile industry to find technical solutions which provide optimal and cost-efficient balance between driveability and fuel efficiency within the boundaries set by emission legislation [1] [2]. A full replacement of fossil fuel driven internal combustion engines in the transportation sector with completely renewable energy sources require several decades to find durable and affordable alternatives to current vehicles. However, a partial replacement of internal combustion engines with electric motors, i.e. hybrid vehicles, is considered as an acceptable short and a midterm solution which provides improved overall fuel economy and performance and reduced CO_2 emissions. Several vehicle OEMs (original equipment manufacturer) are developing different types of hybrid vehicles (hybrid electric vehicles and plug-in hybrid vehicles) as one of the pathways to continuously reduce fuel consumption of the product line-up [2]. The hybridization of the driveline allows a downsizing of the engine and improves the fuel economy for the vehicle.

A typical hybrid driving cycle involves periods where the vehicle drives only on electricity with the internal combustion engine (ICE) shut off. During this time, both the engine and the exhaust aftertreatment system (EATS) lose heat [3]. This cooling off can affect the ability of the system to be emission compliant. Although the amount of emitted tailpipe pollutions from hybrid vehicles is significantly lower than the corresponding amounts of emissions from conventional vehicles if assuming the same driving cycle and pattern. The exhaust aftertreatment of hybrid vehicles is challenging for other reasons such as the high frequency of start and stop of the engine due to the change of power source and engine conditions. In such circumstances, the temperature of the EATS system decreases significantly in many cases to levels below the ignition temperature of the catalysts in the exhaust aftertreatment system [4]. As a consequence, the EATS components work in failure zones and emission reduction to legislation levels become difficult to meet. Those, new innovative systems and solutions are needed to meet the stringent legislations demands.

The existing Euro VI EATS system consists of three main parts, a diesel oxidation catalyst (DOC), a diesel particulate filter (DPF) and a selective catalytic reduction catalyst (SCR) using urea as a precursor for ammonia which is the reducing agent. Initial engine bench and on-road tests have shown that the most challenging issue in the aftertreatment of emissions from hybrid and plug-in hybrid

vehicles is NO_X conversion. There is great evidence that the existing EATS systems will not be able to work properly under all conditions for the hybrid and plug-in hybrid vehicles.

This master thesis consists of a thorough analysis of test data (engine settings, temperatures, mass flows, emission concentrations, etc.) obtained from engine bench tests of plug-in hybrid engine set-up in combination with Euro VI EATS system and on-road tests of hybrid and plug-in hybrid vehicles equipped with Euro V EATS systems. The test data analysis will help to understand the impact of the hybrid system operation conditions on the performance of the EATS system. The output of this work will be used as input for further analysis that are needed to define guidelines for the design and control of EATS systems, which are emission compliance in hybrid driving cycles.

1.2 Objectives of the thesis

The main objective of this project was to study the performance of exhaust aftertreatment systems (EATS) during prevailing operation conditions for hybrid and plug-in hybrid electric buses. An analysis of the gathered data will be performed to determine the specific levels in g/kWh for each legislated emission and identifying the bottlenecks in the current EATS systems when they fail to meet the legislation targets.

2. Commercial Vehicle Hybrid Powertrains

Hybrid vehicles combine two or more power sources in the drivetrain. The main drive system in the current commercial hybrid vehicles is an internal combustion engine (ICE) while electric motors are most often used as the secondary power source. A few demonstration hybrid vehicles consist of an ICE and a fuel cell system (FC). The main driving force for the development of the hybrid vehicles is to improve the fuel efficiency, reduce fuel consumption and/or reduce the emission of harmful pollutants. The improved energy efficiency in hybrid vehicles is achieved by recovering and storing the kinetic energy during regenerative braking and use this energy when needed in an optimal way [2].

2.1 Energy Storage systems

Hybrid vehicles can be classified based on the utilized energy storage technique. These energy storage types are briefly described below:

2.1.1 Electric Hybrid

Power generation in hybrid-electric powertrain is achieved by combining an internal combustion engine propulsion system with an electric propulsion system. In these types of powertrains, the kinetic energy of the vehicle is converted into battery-charging electric energy through regenerative braking, instead of wasting it as heat energy [2].

2.1.2 Hydraulic Hybrid

In this type of powertrains, the kinetic energy is captured through regenerative braking for the hydraulic hybrid vehicle. The system contains a hydraulic pump and a reservoir to a hydraulic accumulator. When the vehicle slows down, the pump becomes activated and moves fluid from the reservoir to the hydraulic accumulator and hydraulic pressure in the accumulator builds. The compressed gas stores energy and can power a hydraulic motor to propel the vehicle [2].

2.1.3 Pneumatic Hybrid

The pneumatic hybrid powertrain uses the engine to convert braking energy into compressed air, which can be stored in an on-board air tank [5]. The stored energy in the compressed air is then used to power the vehicle to reach the cruising speed before switching on the conventional combustion engine

2.1.4 Mechanical (Flywheel) Hybrid

The kinetic energy during the regenerative braking in this type of powertrains is stored in a high-speed flywheel. The flywheel hybrids do not require any energy conversion but generally yields lower efficiencies compared to battery-based systems because of energy losses caused by bearing friction[2].

2.2 Hybrid architecture

The most common types of hybrid design architectures are described below:

2.2.1 Parallel Hybrid

The primary power system in parallel hybrid vehicles is an internal combustion engine and the secondary power source is often an electrical motor connected to a mechanical transmission [1.26].

The electric motor is located between the combustion engine and the transmission and it is connected to a Li-Ion battery or another energy storage system. The efficiency gain in these vehicles is higher than in conventional vehicles since some of the vehicle accessories are powered by the electric motor, which means that these accessories run at a constant speed, regardless of how fast the combustion engine is running. When the two power sources are mechanically coupled on the same axis, the speeds at this axis must be identical and the supplied torques is added together. When one of the two sources is used, the other must either also rotate in an idling manner or be connected by a one-way clutch. The portion of power provided by either one of the power sources varies. In some systems, the combustion stands for the major part of power demand, while the electric motor is used only when a boost is needed or vice versa. The system is designed in such a way that the two power sources can power the vehicle individually or together [2].

2.2.2 Series Hybrid

Series hybrid vehicles are propelled by the electric motor which is powered by the internal combustion engine via an electric generator. The electric power from the electric generator can also be used to charge the energy storage system in the vehicle. At high speed and torque demand, the electric motor draws electricity from the system batteries, capacitors, and the electric generator.

In a series hybrid hydraulic system, the energy is transferred from the engine to the drive wheels through hydraulic power. This system type is suitable for operation conditions with many stop-and-go duty cycles [6]. Energy recovery and storage in these vehicles is handled by hydraulic pumps and hydraulic storage tanks. This technology has a significant potential for fuel efficiency improvements and emission reductions in some driving cycles. Fuel economy improvements are achieved by operating the engine in a more efficiently manner by for example shutting down the internal combustion engine (ICE) when not needed. The efficient use of the braking energy which otherwise is wasted in conventional vehicles further improve the fuel economy [2].

2.2.3 Power-split Hybrid

This technology is a combination of series- and parallel hybrid technologies. By incorporating a power-split device, it becomes possible to power the wheels either mechanically via the combustion engine or electrically via the electric motor. In a conventional vehicle a larger engine is needed to provide the required torque at lower engine speeds to accelerate the vehicle from a standstill condition. However, the larger engine has a higher power output capability than needed for steady speed cruising which is a sort of capacity waste. On the other hand, the maximum torque for the electric motor is at the standstill condition. Thus, the combination of conventional combustion engine with electric motor provide the possibility for energy efficiency improvement.

In addition to the internal combustion engine, there is a need for two motors or pumps. One motor is used as a generator while the other one is used as a motor and generator. The two motors are connected through a planetary gear set and controlled by a powertrain controller [2].

2.2.4 Plug-in Hybrid-electric Vehicle (PHEV)

The PHEV provide high energy storage capacity and can be designed either as a parallel or series hybrid system depending on the application. The energy storage system of a PHEV can be charged by either connecting it to an electricity supply source or by using the on-board internal combustion engine. As the ICE is used less in PHEV, the amounts of produced on-board emissions are less than

other types of hybrid vehicles. The operating cost for PHEV is reduced as long as the electricity used is cheaper than the corresponding amount of gasoline or diesel fuel needed for the production of equal amount of power. Further, this type of systems provides a quiet working environment for a utility service truck. For a plug-in hybrid utility service truck, the powertrain system can be designed to provide power for application use during ICE-off operations [2].

3. Diesel combustion

In a diesel combustion engine diesel fuel is injected as a spray with small droplets to be mixed with compressed air which is trapped in the combustion chamber [7]. The ignition is caused by the heat exchange between the diesel fuel and the compressed air. Since the reaction occurs at gas phase, it is essential that the liquid diesel is rapidly evaporated before the oxidation reaction with air. Diesel combustion engines are characterized by high thermal efficiency. The technology has been a subject to optimization since the invention of the diesel engine (1894 by Rudolf Diesel), which has resulted in improved fuel efficiency and a dramatic reduction of the amount of produced NO_X.

3.1 Emissions formation

3.1.1 NO_X formation mechanisms

In an internal combustion engine energy is derived from the burning of fuel in air, resulting in the formation of product gas which consists mainly of CO_2 and water vapour in addition to the N_2 from the air. Under the prevailing conditions in the combustion chamber, some of the N_2 is oxidised, leading mainly to the formation of NO. NO formation in the combustion chamber is favoured by high temperature and pressure and when oxygen is in excess (lean conditions). The formation of NO has been explained by two main mechanisms: (i) the Zel'dovich or the thermal mechanism, which is the path where the major fraction of NO_X is formed and (ii) the prompt mechanism [Heywood JB] where a small amount of NO is formed from the chemically bounded nitrogen in the fuel. Reactions 1 -3 show the thermal mechanism [8]:

$$N_2 + O \rightarrow NO + O \quad (1)$$

$$N + O_2 \rightarrow NO + O \quad (2)$$

$$N + OH \rightarrow NO + H \quad (3)$$

NO formation is controlled by reaction (1) which is the rate-determining step. The activation energy for this reaction is high influencing the amount of NO which is formed. The prompt-NO mechanism produce NO earlier in the flame than the thermal mechanism

3.1.2 Particulate Matter (PM) formation

One by-product of non-complete diesel oxidation in the combustion chamber is the formation of soot. The non-complete oxidation occurs in the rich zones of the combustion chamber. Particles are then formed from the soot after a certain time through several steps. The process starts with the pyrolysis step where hydrogen atoms from the fuel detach from the fuel molecules and become precursors for the formation of poly-aromatic rings. The poly-aromatic rings then build three dimensional structure sheets, forming primary carbon particles. This phase in the process is called the nucleation phase. The nucleation phase is followed by a surface growth step where additional aromatics, built from the acetylene which is formed on the rich side of the flame, attach to the primary particles. After a short time period additional hydrocarbon condense on the particle surface and finally the formed primary particles agglomerate to large complex structures [9].

3.1.3 NO_X - PM trade-off

The temperature in the combustion chamber of diesel engines play a significant role on the amount of formed NO_X and PM. Soot particles which heavily contributes to the total mass of PM, are oxidized at the boundary of the diffusion flame sheath at elevated temperatures resulting in a reduction of the total PM mass. However, higher temperatures favour the formation of NO_X. Hence decreasing the temperature by means of any method to suppress the formation of NO_X will result in an increase of total amount of PM. This dilemma is called the NO_X – PM trade-off [10].

3.2 Emissions regulations

Emissions standards have been set-up and gradually tightened since the early 90s to reduce the amount of released air-borne pollutants to the environment from automobiles, power plants and factories. The regulation standards are managed differently in different countries and regions in the world. Vehicle emissions standards in Europe are set-up by the European commission, while the corresponding standards in the US are managed by the Environment Protection Agency (EPA) [11]. State and local governments are given the possibility to apply for waivers to enact stricter regulations. The California state via the California Air Resource Board (CARB), for example, has set-up more stringent levels than those defined by EPA and several other states in the US have adopted the California state standards. In Japan the emission standards are managed by the Japanese government. Several other countries have implemented restrictions for automotive emissions as US, Europe and Japan by applying either one of these standards.

The current regulated emissions are nitrogen oxides (NO_X), total hydrocarbon (THC), non-methane hydrocarbons (NMHC), carbon monoxide (CO) and particulate matter (PM). These emissions are regulated for most vehicle types, including cars, trucks, trains and construction equipment's [12]. For each vehicle type, different standards apply. Figure 1 gives a summary of global on-road NO_X and PM emission standards for heavy-duty vehicles. Normally, the US standards are expressed in g/bhp-hr, whereas the European and Japanese standards are expressed in g/kWh. However, in this figure all standards are expressed in the same unit (g/kWh).

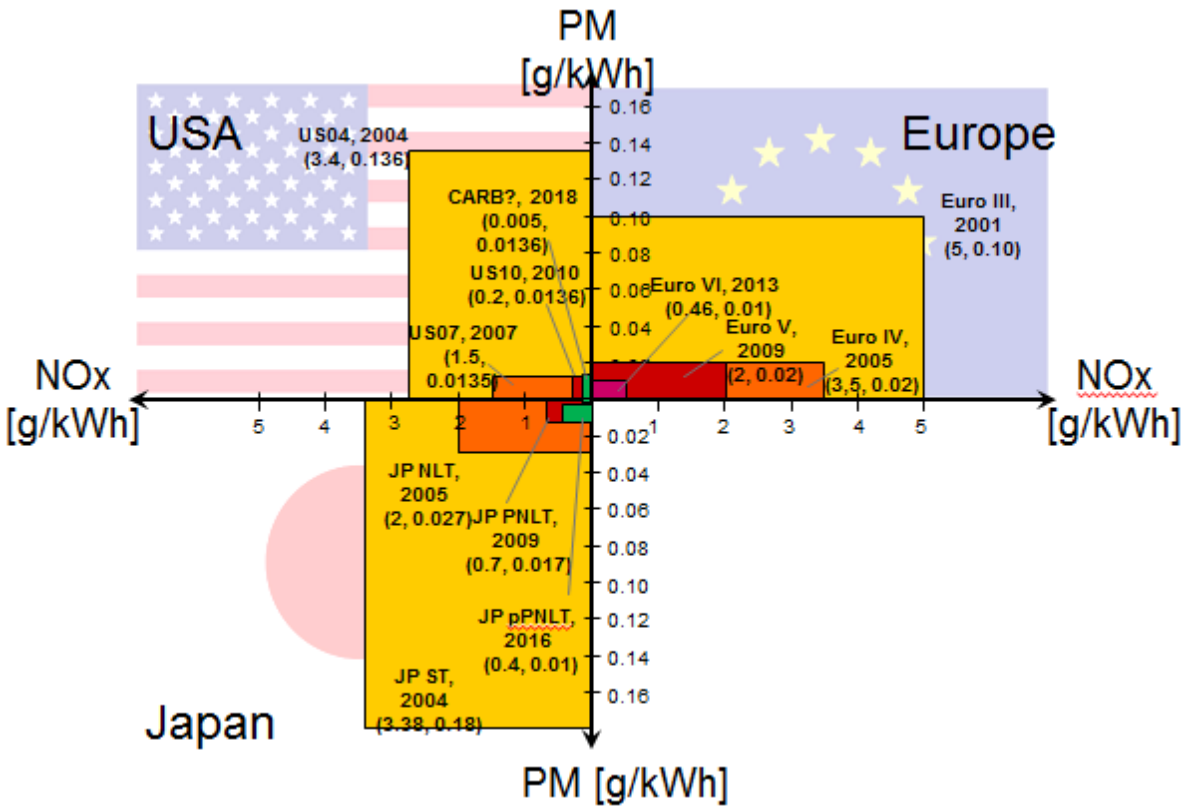

Figure 1: Global NO_X and PM on-road emissions standards for heavy-duty vehicles.

Tables 1 and 2 show summaries of the EU emission standards and their implementation dates for heavy-duty diesel engines steady-state and transient testing, respectively.

Table 1: ***EU Emission Standards for Heavy-Duty Diesel Engines: Steady-State testing*** *[12]*

Stage	Date	Test	CO	HC	NO_X	PM	PN	Smoke
			g/kWh				*1/kWh*	*1/m*
Euro I	1992. ≤ 85 kW 1992. > 85 kW	ECE R-49	4.5 4.5	1.1 1.1	8.0 8.0	0.612 0.36		
Euro II	1996.10 1998.10		4.0 4.0	1.1 1.1	7.0 7.0	0.25 0.15		
Euro III	1999.10 *EEV only* 2000.10	ESC & ELR	1.5 2.2	0.25 0.66	2.0 5.0	0.02 0.10[a]		0.15 0.8
Euro IV	2005.10		1.5	0.46	3.5	0.02		0.5
Euro V	2008.10		1.5	0.46	2	0.02		0.5
Euro VI	2013.01	WHSC	1.5	0.13	0.40	0.01	8.0×10^{11}	

a- PM = 0.12 g/kWh for engines > 0.75 dm^3 swep volume per cylinder and a rated power speed > 2000 min^{-1}.

Table 2: ***EU Emission Standards for Heavy-Duty Diesel and Gas Engines: Transient Testing*** *[12].*

Stage	Date	Test	CO	NMHC	CH_4[a]	NO_X	PM[b]	PN[e]
			g/kWh					1/kWh
Euro III	1999.10 *EEV* 2000.10	ETC	3.0 5.45	0.40 0.78	0.65 1.6	2.0 5.0	0.02 0.16[c]	
Euro IV	2005.10		4.0	0.55	1.1	3.5	0.03	
Euro V	2008.10		4.0	0.55	1.1	2.0	0.03	
Euro VI	2013.01	WTTC	4.0	0.16[d]	0.5	0.46	0.01	$6.0x10^{11}$

a - for gas engines only (Euro III-V: NG only; Euro VI: NG + LPG)

b - not applicable for gas fueled engines at the Euro III-IV stages

c - PM = 0.21 g/kWh for engines < 0.75 dm^3 swept volume per cylinder and a rated power speed > 3000 min^{-1}

d - THC for diesel engines

e - for diesel engines; PN limit for positive ignition engines TBD

Additional provisions of the Euro VI regulation include an ammonia (NH_3) concentration limit of 10 ppm applicable for diesel and gas engines. It is likely that a maximum limit for NO_2 will also be defined in near future.

3.3 Emission control technologies

A variety of engine and after-treatment technologies have been developed to meet the stringent legislation. These technologies are described below:

3.3.1 Control of combustion

The amount of NO formed in a gasoline or diesel engine depends on the combustion which can be controlled to a certain extent by adjusting the engine operation. For example, NO formation may be supressed by retarding the spark timing in gasoline engines and the fuel injection in diesel engines [8]. However, it is more difficult to reduce the amount of NO_X in diesel engines due to the high

combustion temperatures and oxygen-rich operational regime of the engine. Additionally, the effects of engine adjustments are limited due to a trade-off between NO_X and particulate matter (PM). Engine calibration is usually used to maximise the fuel efficiency and balance the PM and NO_X emissions. In some cases, one of the two pollutants are reduced via engine calibration while the other one is reduced using a suitable exhaust after-treatment system.

3.3.2 Exhaust gas recirculation (EGR)

Exhaust gas recirculation (EGR) is a method by which part of the exhaust gas is recirculated a controlled way to the combustion chamber via the inlet system. This method is used for several purposes, mainly to supress the formation of NO_X in the combustion process of light- and heavy-duty engines. EGR technology can -also be used to, among others, boost the vaporization of liquid fuels in spark-ignition engines [13], enable close cycle diesel engines [14] and for improving the ignition quality in diesel engines of some fuels which are difficult to ignite [15]

Mixing exhaust gas with intake air results in a decrease in the oxygen fraction while the fraction of combustion by-products such as CO_2 and H_2O increase. Arconumanis [1] has shown that an increase in EGR from 0 to 50% results in a decrease in O_2 fraction in the inlet gas from 21 to 14% while CO_2 fraction can be about 5% [1]. The decrease in oxygen fraction and increase in non-oxygen molecules with EGR results in a decrease in flame temperature and, thereby, a decrease in NO_X emission. The decrease in flame temperature occurs as the flame in such condition is broadening to pull the required oxygen. This result in an increase of non-oxygen molecules in the broadened flame zone and these molecules absorb heat from the flame and lower the flame temperature. This effect can be referred to the as dilution effect.

The temperature decrease is also to a certain extent a consequence of a series of heat consuming reactions, such as the dissociation of diluent gases (CO_2 and H_2O). The heat absorption of non-reacting gases increases with higher EGR rate as the mass in the cylinder increase (also called added-mass effect). Another influencing factor is the average heat capacity which also increases with the EGR rate as both CO2 and H2O have higher specific heat than air (“thermal effect”). A further decrease in temperature is achieved by EGR cooling using a suitable type of heat exchanger. The temperature in the combustion chamber decreases as more heat is absorbed by the gas flow. The expression for the increase in heat absorption of non-reacting gases, ΔQ, is presented below in eq. A1, in the appendix section.

Unfortunately, the application of EGR for NO_X emission reduction is not only of advantages. While NO_X emissions are reduced with the aid of EGR technology, PM emission is increased since EGR supresses the flame speed significantly resulting in an incomplete combustion [12].

3.3.2.1 High Pressure Loop EGR (HPL EGR)

In this EGR configuration, a portion of the exhaust flow upstream of the exhaust gas turbine is cooled in a heat exchanger (EGR cooler) and then injected into the intake manifold downstream the compressed intake air through an electronically-controlled EGR valve. This approach is commonly referred to *as high pressure loop (HPL) EGR or as short-route (SR) EGR*. One drawback with HPL EGR systems is the increased fuel consumption penalty, especially at high engine loads [12].

3.3.2.2 Low pressure Loop EGR

This EGR system uses exhaust gas that has been filtered through, i.e., the exhaust gas which exits the turbine is filtered in a diesel particulate filter before entering an EGR cooler. The cooled filtered exhaust gas is mixed with the intake air and the air/exhaust gas mixture is pressurized in the compressor and cooled in a heat exchanger before being introduced into the engine. In this way all the exhaust is utilized in the turbine which is a good way to preserve the turbocharger. At this location, exhaust gas pressure is at a lower level than that of the intake manifold. The challenges that are faced with this configuration is related to difficulties in achieving accurate control of EGR rate during engine load and speed changes, non-complete filtration of the exhaust gas the filter trapping efficiency is less than 100%, carbonaceous and other unfiltered matter flowing through the compressor may be trapped in the narrow cooler passages, and condensate development when EGR temperature drops [12].

3.3.2.3 Hybrid pressure Loop EGR

This system is a combination of HPL and LPL EGR. It is used to meet the stringent emission standards. As HPL EGR systems impose an increased fuel consumption penalty, especially at high engine loads and since lower NO_X limits demand higher EGR rates, one potential solution is to use hybrid or dual-loop system where the LPL is used at high engine loads and the HPL at lower engine loads and some combination of the two in the transition region [16].

3.3.3 Turbocharger

A turbocharger which consists of a compressor and a propelled turbine is used to increase the engine power output by allowing more air and fuel into the engine cylinder. The turbine which generates mechanical power from the exhaust gas is used to drive the compressor and the compressor is used to increase the air density by increasing the intake pressure of the air[12].

3.4 Exhaust aftertreatment techniques

3.4.1 Diesel Oxidation Catalyst

A diesel oxidation catalyst (DOC) is present in most modern after-treatment system operating under lean conditions [17]. This kind of catalyst can successfully convert two of the three main pollutants, CO and hydrocarbons (eq. 4 and 5) [18]. Both the structure and configurations is similar to that of the TWC, however the DOC is not capable of reducing NO_X [19]. The excess of air under lean-conditions leads to near complete oxidation (above 95%) of CO and HC which leaves inadequate amounts of reactants for converting NO.

Modern DOCs are usually based on cordierite (ceramic) monoliths. A high surface area material, called a washcoat is adhered to the monolith surface. A suitable precious metal, most commonly Pt, Pd or a combination of both, are dispersed on the high surface area washcoat. The most widely used washcoat supports are made-up by alumina, Zirconia, silica or zeolite [17] . The usual catalyst substrate size for diesel truck applications are 180-250 mm in diameter and 150-180 mm in length. The platinum group metal (PGM) loading on the DOC depends on the level of emission control, 80-100 g/ft3 is needed for PM, HC and CO control at low temperature [20].

The reaction of NO to NO_2 takes place inside the DOC, this oxidation is a crucial step in passive soot trap regeneration and in having a sufficient NO_X reduction process [19]. Typical NO_2/NO_X engine-out ratios range from ~10% which can be compared with post DOC levels of up to 50%. The nitric oxide oxidation is dependent on temperature, oxygen concentration and precious metal dispersion. A portion of the liquid hydrocarbons on the soot (soluble organic fraction, SOF components) are also oxidized over the DOC [17] Since liquid hydrocarbons is normally trapped on the DPF it is seen as PM and thus a lowering of PM is accomplished over the DOC[17].

Oxidation reactions are exothermic and therefore increase the surrounding temperature. An after-treatment hydrocarbon injector (AHI) is positioned upstream from the DOC to generate extra heat from fuel oxidation. This component feature is essential in order to supply the necessary heat for active regeneration of the downstream DPF component.

The reaction mechanism for both CO and HC oxidation follow Langmuir-Hinshelwood, where adsorbed oxygen reacts with either adsorbed HC or CO. The surface reaction is the rate-determining step [17].

$HC + O_2 \rightarrow CO_2 + H_2O$ (4)

$CO + 1/2O_2 \rightarrow CO_2$ (5)

3.4.2 NO_X reduction

Selective catalytic reduction (SCR) is currently the leading technology that can be applied to control NO_X emissions and enable diesel vehicles to comply with the stringent emissions standards [21]. The SCR technology is based on injecting a certain reducing agent upstream of the SCR catalyst to selectively reduce the NO_X over the catalyst to N_2. The type of reducing agent used in combination and catalytic material are two important aspects which determine the suitability of the SCR system for a given application. Selective catalytic reduction of NO_X can be achieved either by using hydrocarbon (HC-SCR), for example, the on-board fuel or ammonia (NH_3-SCR) as the reducing agent. Although the HC-SCR technology has been subject for research in many years, the technology is still suffering of many limitations which obstacle its introduction into real world applications in the automotive industry. The main reason is poor performance of the available HC-SCR catalyst at low temperatures. In contrast, NH_3-SCR has been the method of choice for NO_X reduction by most vehicle manufacturer. It is worth to mention that NO_X reduction technology is chosen on the basis of the total system cost (catalyst, reducing agent, system auxiliaries, maintenance, etc.), controllability, as well as system size and volume. Time has shown that NH_3-SCR is the winning concept among other NO_X abatement technologies such as EGR and NO_X adsorber catalysts.

The NH_3-SCR method is based on injecting the ammonia (NH_3) forming reducing agent, aqueous solution of urea ($CO(NH_2)_2$) into the exhaust stream to chemically reduce NO_X into nitrogen. The ammonia is generated via thermolysis reaction once mixed with the hot exhaust gas where the temperature is preferably above 200 °C (eq.6) and hydrolysis (eq.7), where the hydrolysis reaction may take place either over a separate catalyst or on the SCR catalyst itself (Gieshoff 2001) or on the inlet part of the SCR catalyst [22].

$CO(NH_2)_2 \rightarrow NH_3 + HNCO \ \ (thermolysis\ of\ urea)$ (6)

$HNCO + H_2O \rightarrow NH_3 + CO_2 \ \ (hydrolysis)$ (7)

$4NH_3 + 3O_2 \rightarrow 2N_2 + 6H_2O \ \ (ammonia\ oxidation)$ (8)

The first SCR catalyst which was used for mobile application was a vanadia supported on titania [23]. However, the use of vanadia-based catalysts has been limited due to low NO_X reduction performance at low and high temperatures and also because of the toxicity of volatile vanadia. In contrast, metal oxide zeolites such as copper [24-30] and iron [23] have been widely used for SCR application by many vehicle manufacturers since these catalysts have demonstrated high NO_X conversion activity at a wide temperature range.

A number of chemical reactions occur in the ammonia SCR system, as shown in eq. (9) to (13).

$$6NO + 4NH_3 \rightarrow 5N_2 + 6H_2O \quad (9)$$

$$4NO + 4NH_3 + O_2 \rightarrow 4N_2 + 6H_2O \quad (10)$$

$$6NO_2 + 8NH_3 \rightarrow 7N_2 + 12H_2O \quad (11)$$

$$2NO_2 + 4NH_3 + O_2 \rightarrow 3N_2 + 6H_2O \quad (12)$$

$$NO + NO_2 + 2NH_3 \rightarrow 2N_2 + 3H_2O \quad (13)$$

All of these reactions show desirable reaction products (N_2 and H_2O). Eq. (10) represents the standard reaction [31], while eq. (13) is the fast SCR reaction which is responsible for the promotion of low temperature SCR by NO_2 [32]. Since the NO_2 concentrations in the diesel exhaust are low, the NO_2 levels in exhaust aftertreatment systems are purposely increased using an oxidation catalyst upstream the NH_3-SCR to enhance NO_X conversion at low temperatures.

3.4.2.1 Urea injection:

The system consists of a urea tank from which the urea is pumped into an atomizing nozzle which sprays the urea as small droplets into the exhaust gas stream. To achieve high NO_X conversions, it is crucial that the urea droplets are thoroughly mixed with the exhaust gases to form a uniform flow distribution. One way to obtain a good mixing is to use a properly designed mechanical mixer which can be placed in an optimal distance upstream the catalyst. Accuracy and reproducibility of the urea injection are other important areas where SCR performance improvement can be achieved.

The NH_3-SCR system performance is significantly influenced by the urea injection system and the revealing physical and chemical processes in the mixing zone upstream the catalyst. Urea decomposition at temperatures below the urea melting point which is approximately 134 °C (or below 175 °C at extremely low vapour pressure) under normal operating conditions, results in the

formation of many undesired components which result in the formation of solid substances that accumulate in the SCR system and deteriorate the catalyst performance. Thus, urea injection controller becomes a necessity to monitor the exhaust gas temperature and close the urea supply when the temperature drops below a predetermined value also known as the urea dosing temperature, somewhere between 150 and 300°C depending on the catalyst type and configuration. This to prevent catalyst deactivation and secondary emissions that may occur at low temperatures [33].

To meet the stringent emission standards, system control strategies require the utilization of NO_X sensors of 40-20 ppm NO_X sensitivity and little cross-sensitivity to NH_3 [33]. The ZrO_2-based electrochemical sensors are the most common in-situ NO_X sensor which operate quite similar to oxygen sensors in gasoline three-way catalyst systems [34].

3.4.2.2 By-product formation

The operation of diesel engine under transient duty cycles with great variation in mass flows and exhaust temperatures makes it challenging to control the SCR process for the desired reactions only. There is a number of undesirable unregulated and secondary emissions such as NH_3 slip, nitrous oxide (N_2O), hydrogen cyanide (HCN) and various urea decomposition products that may be produced in SCR catalyst systems under various transient conditions. Progress made in the ammonia dosing equipment made it possible to lower the ammonia slip to very low levels (ca 10 ppm) with or without an ammonia slip oxidation catalyst [28]. N_2O emissions in SCR catalyst systems are formed either via the oxidation of ammonia by NO_2 (Eq. 14 and 15), or via the oxidation of ammonia by oxygen (eq. 16). It has been shown that the N_2O emissions increase with temperature and with the SCR catalyst size [35].

$$8\ NO_2 + 6\ NH_3 \rightarrow 7\ N_2O + 9\ H_2O \qquad (14)$$

$$4\ NO_2 + 4\ NH_3 + O_2 \rightarrow 4\ N_2O + 6\ H_2O \qquad (15)$$

$$2NH_3 + 2O_2 \rightarrow N_2O + 3H_2O \qquad (16)$$

The formation of ammonium nitrate and ammonium sulphate at low temperatures is a major problem that affects the NO_X activity and catalyst durability.

3.4.3 Diesel Particulate Filters

Diesel particulate filters (DPF) are devices used to control the emission of the solid fraction of the particulate matter including the elemental carbon from the exhaust of diesel engines. The filtration

efficiency of DPFs is estimated by measuring the particulate mass entering the filter and the particulate mass escaping the filter. There are different types of filtrations techniques, but the most common one is the so-called wall-flow filtration [12]. DPFs of this type are made of high porosity ceramic monoliths with every second channel plugged at the end of the substrate. The particles which enter the filter from the open channels are forced to flow through the walls of the adjacent channels and become trapped in the porous wall material. This is valid for particles which have smaller diameters than the pore diameters. This is called the in-depth filtration. When the pore systems are filled with particles, the particles accumulate on the filter walls (surface storage) to form a soot cake [12]. Particles with large sizes than the pore sizes are also accumulated on the surface. The increase of the filter cake layer thickness results in increased back pressure, which leads to a higher engine fuel consumption. The increase in fuel consumption is mainly due to added mechanical work for exhaust gas compression. Each DPF has a maximum storage capacity and must be regenerated when this level is reached to avoid filter clogging and/or when the pressure drop reaches an unacceptable level from a fuel efficiency point of view.

The DPF regeneration strategy can be designed to remove the trapped soot from the DPF either continuously or periodically. Continuous regeneration occurs by the oxidation of soot with NO_2 which is a stronger oxidation agent than O_2. This strategy requires the formation of NO_2 upstream the DPF by means of a DOC. The periodically regeneration requires an increase of the exhaust gas temperature to levels which realise the oxidation of the accumulated soot. The increase of exhaust temperature is achieved by the exothermic oxidation reaction of injected diesel in the exhaust flow upstream the DOC catalyst. A careful control strategy is needed for the periodic regeneration to avoid rapid temperature escalations to extreme levels which may damage the filter substrate.

Particulate matters contain incombustible inorganic ash particles that originate from substances added to lubricating oils and the fuel for property improvements. These incombustible particles cannot be removed from the filter through thermal regeneration [36] . With time, the accumulation of soot, in particular when the periodical regeneration strategy is used, result in the formation of plugs in the filter channels and result in a gradual increase of the back pressure. Dedicated maintenance procedures, such air blowing with compressed air or washing with water, are required to clean the DPF from ash.

3.5 Exhaust aftertreatment Systems (EATS)

The conventional diesel engine has been optimized significantly through the years in order to improve the fuel efficiency and reduce the amount of harmful emissions. The concept of NO_X-PM trade-off has been used both for light-duty and heavy-duty vehicles to reduce the amount of either NO_X or PM. Diesel injection timing is/has been one of the employed strategies in this context. For NO_X control, retarded injection timing is one way to go, although to a certain limit in order to avoid unacceptable PM emissions. Turbocharged diesel engines also provide a possibility to reduce the amount of formed NO_X compared to naturally aspirated engines. The emissions can be further reduced by the introduction of turbocharged and after-cooled diesel engines and through electronic engine control [10].

The NO_X-PM emission trade-off has shown to be important for the design and integration of aftertreatment strategies with the diesel engine as this technology provides the possibility to utilize the aftertreatment system for controlling only one of the pollutants, while the other can be controlled in-cylinder. There are two possible design alternatives:

1. Low NO_X engine calibration with PM emission aftertreatment: A diesel particulate filter system can be used to control increased PM emissions that result from low NO_X engine design.

2. Low PM engine strategy with a NO_X control device: Here a NO_X aftertreatment device is used to reduce the high amount of NO_X as a consequence of engine calibration for low PM. An example of this is the urea-SCR used to control NO_X from the heavy-duty Euro V engines without the need for PM aftertreatment as illustrated in Figure 2.

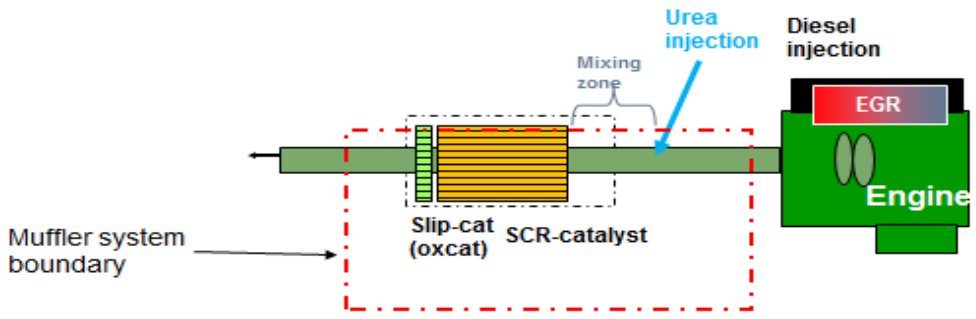

Figure 2: System Layout for Euro V.

3.5.1 EATS for conventional vehicles

The limits for NO_X in Euro IV and Euro V NO_X are 3.5 and 2 g/kWh, respectively. By using the urea-SCR technology and calibrate the engine for low PM, it has been possible to meet the Euro IV and Euro V limits for both NO_X and for PM [24]. This has also provided the opportunity to reduce the size, cost and complexity of the aftertreatment system by eliminating the need for the DPF. However, when the emission demands increase as in Euro VI, the exhaust aftertreatment system becomes more complicated, partly because both DPF and NO_X reduction devices will be required (see Figure 3) to meet the targets (0.01 g/kWh and 0.46 g/kWh, respectively), but also the high NO_X reduction requirements demands further catalyst technology improvements. A more sophisticated urea injection system in addition to the necessity of combined SCR with EGR in order to reach satisfactory low NO_X tailpipe limits. The transient operation present further challenges on the EATS system where, among others, the control of the ammonia slip and other secondary emissions become a challenge and may require a closed-loop NO_X feedback system. Progress in NO_X sensor technology is needed to make such systems possible.

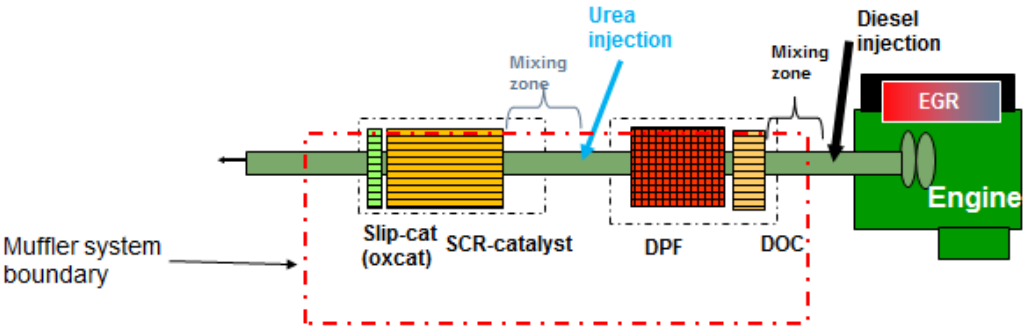

Figure 3: System Layout for Euro VI

3.5.2 EATS for hybrid vehicles

The exhaust aftertreatment system for hybrids consist of the same components as for the regular diesel vehicles but the performance of the system may be different since the operating conditions change between the hybrid solution and the conventional vehicle. Since the start and stop frequency of the ICE in hybrid vehicles are high, the temperature of the EATS will be low, sometimes below the ignition temperature for the aftertreatment devices. This may lead to unacceptable tailpipe levels of CO, HC or unconverted NO_X. The urea system will not inject urea if the temperature is below the dosing temperature thus causing a shortage of reactants in the exhaust flow entering the SCR-catalyst and thereby also limiting the possibility of storing ammonia in the catalyst. This problem is more severe for PHEV since the electric system has the ability to supply power more frequently and with longer duration.

4. Test procedures

4.1 On-road tests with hybrid and conventional diesel bus

Three city buses are used as test vehicles in this measurement, one reference standard diesel bus and two hybrid busses. The on-road cycle tests are performed during two occasions, summer and winter. The average ambient temperature during summer was 18 °C and 1 °C during winter. The difference in weather condition was considered a relevant factor for the EATS performance. The same reference bus, presented in table 1 is used during both summer and winter while hybrid bus FT7 is used during summer tests and hybrid bus SD2 during winter (see table 2 and 3). The weight of the vehicles used in these measurements is at half load. The reference bus has a 9l engine and the hybrid buses a 5l internal combustion engine. The change of hybrid bus during the two occasions was not deemed to influence the fuel consumption and emission results and they are henceforth simply referred to as the hybrid bus or HEV. The EATS is a Euro V system which contains a SCR-catalyst and an ammonia slip catalyst (ASC).

To evaluate fuel consumption and emission levels for typical city driving the bus route CBR85 also called the City 2 cycle were used. The cycle with a total distance of 23 km contains both urban and suburban parts and takes approximately 4000 s to travel. The test vehicles stop at each bus stop for 15 seconds in order to simulate passengers getting on and off the bus.

For measuring the fuel consumption flow meters are mounted on the fuel pipes from the fuel tank and a FTIR is used for analyzing the engine exhausts. There was one FTIR available to measure the tailpipe emission for each cycle test run. In order to calculate an approximate NO_X conversion one test run were performed using the FTIR to determine the engine out emissions by having the measurement point before the EATS.

In the result section for the CBR85 route some additional evaluation on the urban and suburban parts of the cycle are investigated to see how driving patterns influence the emission levels and fuel consumption. The urban part with more stops had an average speed of 16 km/h compared to the suburban part with an average speed of 22 km/h.

Table 3: ***Reference bus, B014, specification***

Unit	Type/model	Data
Bus ID	B014	Flower power
Bus type	7700	
Chassis ID	114449	
Engine	D9l	Euro 5, 230kW
Vehicle weight	Half loaded/Empty	14500/12500kg

Table 4: ***Hybrid bus, FT7, specification***

Unit	Type/model	Data
Bus ID	FT7	
Bus type	7700	
Engine	5L	Euro 5 160kW
Vehicle weight	Half loaded/Empty	14500/12700kg
Electric motor	I-SAM	70kW cont, 120kW peak
Battery	MAGNA	1kWh, 90kW

Table 5: ***Hybrid bus, SD2, specification***

Unit	Type/model	Data
Bus ID	SD2	
Bus type	7700	
Engine	D5L	Euro 5 160kW
Vehicle weight	Half loaded/Empty	14500/12700kg
Electric motor	I-SAM	70kW cont, 120kW peak
Battery	MAGNA	1kWh, 90kW

A rig test series, SORT1-3, were also added to this evaluation in order to further investigate driving pattern impact.

Standardized On-Road Test Cycles – SORT

A driveline was installed in the test cell ML2 at Volvo Technology at Johanneberg Science Park. It consisted of a 5 litre diesel engine (Euro VI) with a dual clutch gearbox. On the gearbox the electric motor is located together with a reduction gear to the power take off. A battery, an electric motor drive, double DC/DC and two TVD (Traction Voltage Distribution) were also included in the driveline.

The SORT cycles were designed to get a reproducible test method for on-road tests of buses in order to measure their fuel consumption. Three different SORT cycles have been tested and they have been defined for three different operating patters:

- SORT1 = urban driving – average speed: 12.3 km/h
- SORT2 = mixed driving – average speed: 18.9 km/h
- SORT3 = suburban driving – average speed: 26.1 km/h

One reason for developing the SORT cycles is to get a common on-road test procedure that can be used to compare different buses when it comes to fuel consumption and emissions.

4.2 On-road tests with plug-in hybrid bus

A new plug-in hybrid bus, Hyperbus 7900 was tested between 8-11 of September in 2013 on the bus 60 route cycle in Gothenburg, going from the bus stop Redbergsplatsen to Masthugget and then back again to Redbergsplatsen. The average ambient temperature during these test days were 15°C. The distance of the relatively urban cycle is approximately 17 km and takes around 4400s to complete. The cycle run were performed 5 times in order to get reproducibility.

The bus is a parallel PHEV operating with an electric engine and a 5l ICE. The EATS consist of a SCR-catalyst and an ASC-catalyst (Euro V) and the ICE is of Euro VI type.

Two FTIRs were installed to measure engine out and tailpipe emissions simultaneously, the Urea dosing system did however malfunction and no urea were injected. Since no relevant activity was observed over the SCR-catalyst due to the absence of urea the second FTIR was removed and only engine out was measured. A thermocouple was installed upstream the SCR-catalyst to measure the temperature.

4.3 Rig tests with MD plug-in hybrid vehicle

During 4 different days in 2012 at the 14th of June, 30th of August and 7-8th of November a total of 13 cycle test were performed on an engine rig at a Volvo site in Ageo, Japan. The cycle tests were performed in the following order:

- 14th of June – Comparison between PHEV and HEV on the City 1 cycle: 1 PHEV test using heat modes, 1 PHEV test without heat modes and 1 HEV test
- 30th of August – 4 PHEV City 2 cycle tests
- 7th of November – 3 PHEV City 1 cycle tests using heat modes
- 8th of November – 3 PHEV City 1 cycle tests without heat modes

The EATS is of Euro VI type and consists of DOC, DPF, SCR and an ASC-catalyst. The engine is a Euro VI, 5 litre ICE named B5L SD.

5. Results and Discussion

Results and data that Volvo AB considered sensitive and confidential have in table form been normalized and in some figures axis and values are hidden.

During the entire result section the calculated specific standards in g/kWh will solely be based on the amount of energy produced by the ICE and not by the electric motor. This method of determining the specific emission levels is more stringent as the electrical energy produced is excluded and thereby more emissions needs to be reduced through the EATS. The molecular mass used to determine the specific NO_X levels is 46 g/moles, i.e. the molecular mass of NO_2, since the emitted NO is assumed to be oxidized into thermodynamically more stable NO_2 once released in the atmosphere.

5.1 On-road tests with hybrid and conventional diesel bus

The results from this section is introduced by an overview figure presenting values for all the evaluated test runs performed during both winter and summer.

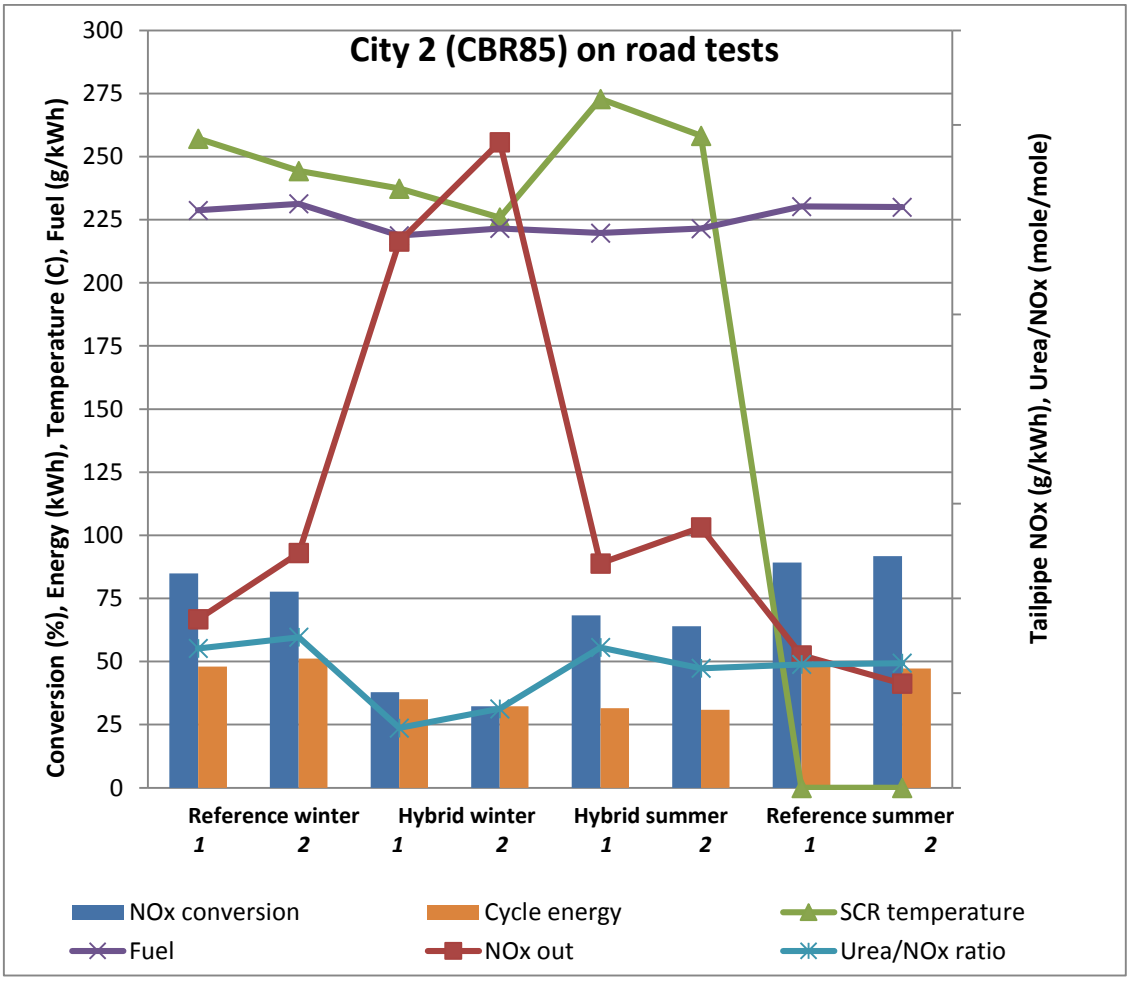

Figure4. Cycle performance data from on-road City 2 tests for HEV and conventional diesel vehicle

This figure compares results from on-road testing during winter and summer for a hybrid bus and a conventional (reference) diesel bus. The winter tests show low NO_X conversion and consequently high specific tailpipe NO_X for the hybrid vehicle while the reference bus has higher conversion and improved Euro V specific NO_X levels for the first cycle test and slightly increasing on the second run. It is vital for the EATS performance that the exhaust gas temperature upstream the urea injection position as well as in the SCR unit is sufficiently high to avoid risk of forming undesirable by-products from urea instead of reducing NO_X. High temperature is also important to achieve high SCR Activity. The Urea/NO_X ratio for the HEV winter tests are below the theoretical ratio of 1 which without stored NH_3 cannot convert the necessary amount of NO_X to reach Euro V levels. During the summer tests the conversion of NO_X is significantly higher for the HEV, most likely as a result of higher SCR temperature and a more suitable Urea/NO_X ratio. The increased conversion is however not enough to reduce the amount of NO_X to the low specific NO_X levels of the reference bus.

The difference in average SCR temperatures between the winter and summer for HEV tests is rather high (~ 50 °C) which indicates that the EATS system had insufficient amount of insulation material to reduce heat losses during colder climate.

The major incentive for hybridization of the drivetrain is the reduced consumption of fuel and AdBlue as can be seen in table 6.

Table6: ***Diesel and AdBlue consumption and engine out emissions for HEV and reference bus on-road winter and summer tests.*** **The specific emission are standardized against reference winter test**

Type	Diesel fuel consumption (l/100km)	AdBlue consumption (l/100km)	Fuel efficiency, η_f (%)	Engine out CO (%)	Engine out CO_2 (%)	Tailpipe CO (%)	Tailpipe CO_2 (%)
Ref winter	57.7	13.9	36.5	-	-	-	-
Ref summer	55.5	13.4	36.4	+230	+19	+70	-4.5
Hybrid winter	37.5	3.8	38.0	-97	+7	-91	-3.5
Hybrid summer	34.8	5.2	38.0	-98.5	+4.5	-99	-3

- ***: data hidden***

The difference in CO and CO_2 levels between the reference and hybrid bus is due to difference in engine type, size and calibration.

In addition to investigating the performance on the City 2 cycle the two buses were also evaluated for urban and suburban driving conditions, see table 7.

Table7: ***Diesel and AdBlue consumption and engine out emissions for HEV and reference bus on-road urban and suburban tests.*** **The specific emission are standardized against reference winter test**

Type	Diesel fuel consumption (l/100km)	AdBlue consumption (l/100km)	Fuel efficiency, η_f (%)	Tailpipe NO_X (%)	Tailpipe CO_2 (%)	Distance (km)	Energy per km (kWh/km)	Mean velocity (km/h)
Ref Urban	69	17.5	35.9	-	-	8.1	2.55	14
Hybrid Urban	37	5	37.4	+36	-2	7.7	1.43	15
Ref Suburban	53	12.5	36.5	-40	-3	19.5	2.02	23
Hybrid Suburban	34	5	38.1	+16	+1	19.1	1.33	23

As shown in table 7, diesel and AdBlue consumptions for both hybrid urban and sub-urban tests are lower compared to those for the reference tests. However, tailpipe NO_X emissions in the hybrid tests are higher than for the reference tests. The difference in energy efficiency between reference bus and the HEV is simply due to the HEVs possibility of using only the electric engine at engine operating points which is deemed to be fuel insufficient, e.g. at idling, where the fuel consumption for the ICE is high in g/kWh. The driving patterns influence on the specific NO_X levels is also less significant for the HEV since the electric engine is working during lower power output periods were cold exhaust would be produced from the ICE.

As an additional measurement the SORT1-3 rig tests were performed for the investigation of driving pattern influence, results are presented in table 8.

Table8: ***Diesel and AdBlue consumption and tailpipe emissions for hybrid bus (?) Sort1-3 rig tests.***

The specific emission are standardized against SORT1.

Type	Fuel consumption (l/100km)	AdBlue consumption (l/100km)	Fuel efficiency, η_f (%)	Tailpipe NO_X (%)	Tailpipe CO_2 (%)	Distance (km)	Energy per km (kWh/km)
SORT1 (urban)	36.3	1.9	32.2	-	-	0.5	1.2
SORT2 (mixed)	28.5	0.7	34.5	+26	-5	0.9	1.0
SORT3 (suburban)	26.9	1.4	35.5	+19	-4	1.5	1.0

The SORT1, urban driving cycle has the highest fuel consumption of the observed cycles, which corresponds to the previously presented results (see table 7). From a fuel economy standpoint the higher velocity driving style seems to be the most beneficial.

NO_X conversion data for these tests, mean SCR temperature, urea/NO_X molar ratios are displayed in table 9. The low NO_X conversion could be due to the low amount of dosed urea and relatively low pre-SCR temperatures during these three cycle tests.

Table9: ***NO_X conversion and relevant parameters for NO_X conversion.***

Type	NO_X conversion (%)	Mean pre-SCR temperature (°C)	Urea/NO_X (mole/mole)
SORT1 (urban)	51.26	200.54	0.49
SORT2 (mixed)	37.15	192.32	0.22
SORT3 (suburban)	40.60	206.58	0.46

5.2 On-road tests with plug-in hybrid bus

The Hyperbus on-road test series were performed to determine engine and EATS performance for a newly developed PHEV on a common bus route in Gothenburg.

Table10. ***Summary data for all 5 on-road Hyperbus tests***

Number of runs	5
Average cycle distance (km)	16,9
Average cycle time (s)	4450
Average speed (km/h)	14,5
Average pre-SCR temperature (°C)	206,5
Average energy electric over cycle (kWh)	13,5
Average energy ICE over cycle (kWh)	7,0
ICE turned off (%)	89,6
Average standstill (%)	25
Average fuel consumed over cycle (1/100 km)	10

It can be demonstrated by table 10 and table 6 that the PHEV consume less fuel than the regular HEV and the conventional reference bus as a result of low usage of the ICE. The route for the Hyperbus tests is different from the CBR85, City 2 route but this significant difference should be an indication for improved fuel economy when employing a PHEV solution.

The average pre-SCR temperature suggests that urea would have been injected if the urea dosing system did not malfunction.

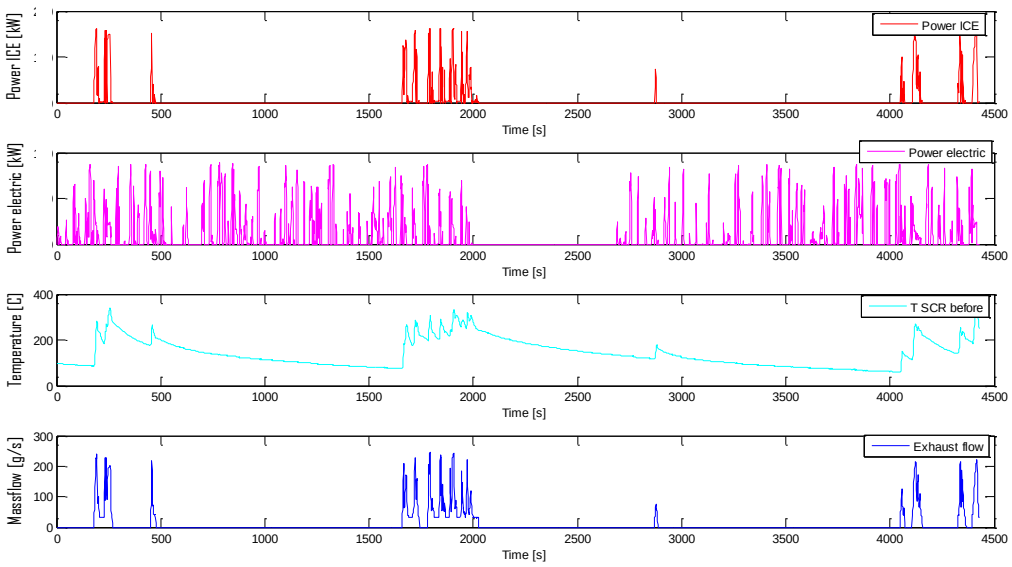

Figure5. Power output, SCR temperature and exhaust massflow plotted against time. Data collected from one of the five hyperbus on-board cycle tests

It is evident from figure 5 that the electrical motor is working a majority of the time when the vehicle is in motion. The ICE starts when the road is inclined to a certain degree, during these periods both engines work simultaneously (i.e. parallel hybrid). The bus has reached the final stop at 2000s and charges the batteries until 2700s. During this time the pre-SCR temperature drops down to about 110 °C from 310 °C.

From figure 5 presented above the pre-SCR temperature is shown during the entire Hyperbus cycle test and in order to investigate the temperature during the different regions were the ICE is working an additional figure is presented below.

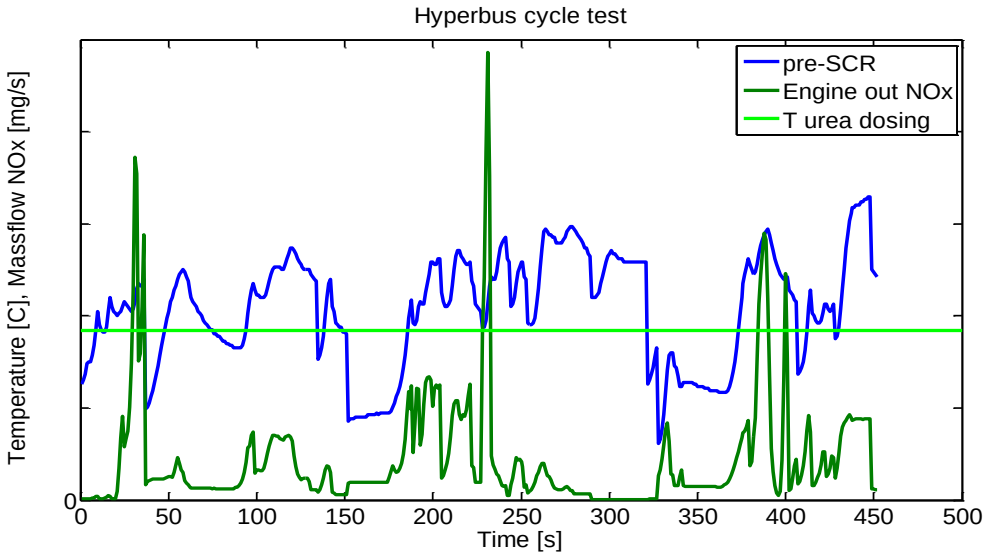

Figure6. Pre-SCR temperature presented along with engine out mass flow of NO_X during the ICE working regions. A straight line showing the minimum urea dosing temperature is also presented

In this figure all the ICE operating regions are put together to outline the total ICE operating time of 452 s. The total mass of NO_X produced from the ICE during this time is 24.24 g, which by EU6 standards of 0.46 g/kWh, would need to be reduced down to 3.29 g by the SCR since the total energy output by the ICE is 7.15 kWh. This NO_X reduction would yield a conversion of 86.4%. The pre-SCR temperature for this cycle test is above the minimum urea dosing temperature for 313 s of the total ICE operating time. This introduces a possible problem when the temperature is below dosing temperature and NO_X passes through the EATS without having urea dosed into the SCR system. As can be seen in the figure the NO_X mass flow is rather low adding up to 2.91 g when the temperature is below the urea dosage temperature, this is a consequence of a relatively low power output by the ICE during these regions. If assuming that no ammonia is stored on the SCR as a consequence of low urea/NO_X ratio the NO_X conversion can be approximated to 0 for the time period of no urea dosing and therefore the NO_X conversion have to increase to 98% on the remaining ICE operating time in order to meet the EU6 NO_X level.

Table11. ***Duration for each period when the ICE is on for one of the Hyperbus tests***

ICE on period	1	2	3	4	5	6	7	8	9	10	11	12	13	14
Duration (s)	188-233	688-804	1003-1028	2103-2194	2242-2263	2311-2323	2383-2420	2477-2508	2704-2709	3973-3990	4002-4078	4278-4286	4293-4309	4360-4380

Table 11 is displaying when each diesel period is occurring, for the 5 hyperbus on-road tests these will obviously vary a bit.

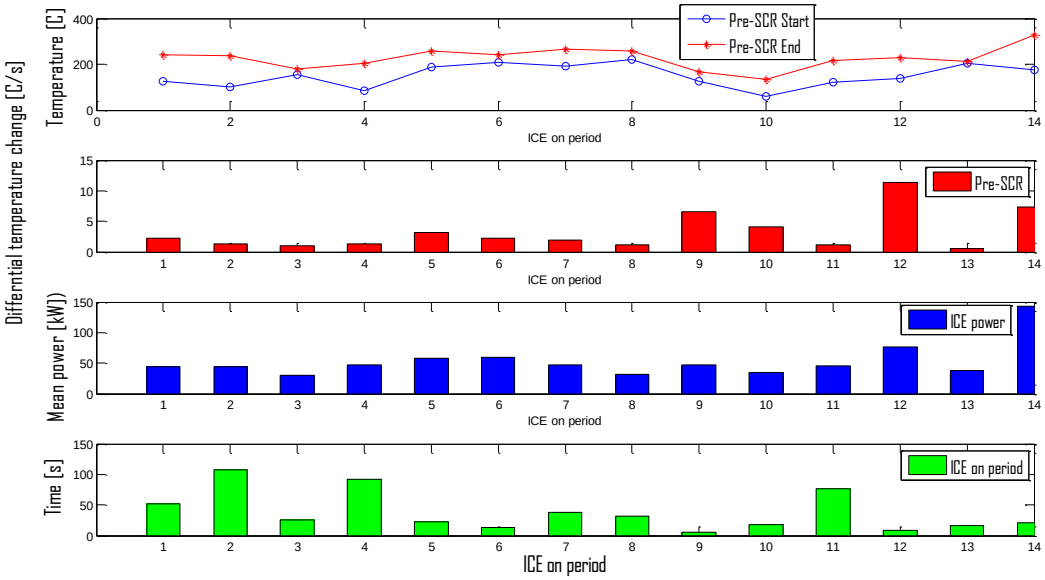

Figure7. Data from one of the hyperbus tests showing values during the different periods when the ICE is on

The SCR temperature change naturally depends on the amount heat generated by the engine which is supplied via the exhaust flow, but also the SCR temperature when the ICE is first ignited i.e. the start at each ICE period. The problem with cold EATS as a consequence of using PHEV was outlined in earlier section (3.5.2), the end temperature at period 1 was 240 °C and the start of period 2 was 99 °C. The system for this vehicle starts injecting urea at 175 °C, therefore large amounts of unconverted NO_X pass through the SCR during the initial part of the "combustion engine period" if no ammonia is stored in the SCR catalyst.

5.3 MD hybrid and plug-in hybrid rig tests

In this section, results from 13 medium-duty plug-in hybrid rig tests performed during a test period of four days are presented and discussed. The engine in these tests is a B5L SD (EU6) and the aftertreatment system used is of Euro VI type. The 13 tests are performed in the following order:

- Tests 1 – 3, plug-in hybrid City 1 cycle with heat mode (WHM)
- Tests 4 -6, plug-in hybrid City 1 cycle without heat mode (WOHM)
- Tests 7 – 10, plug-in hybrid City 2 cycle
- Tests 11 and 12, plug-in hybrid WHM and WOHM on the City 1 cycle, respectively
- Test 13, hybrid electric vehicle on the City 1 cycle for comparison

Figure 8 summarizes NO_X conversion, specific engine-out soot and specific tailpipe NO_X, test start temperature, mean SCR temperature and urea/NO_X ratio for all tests.

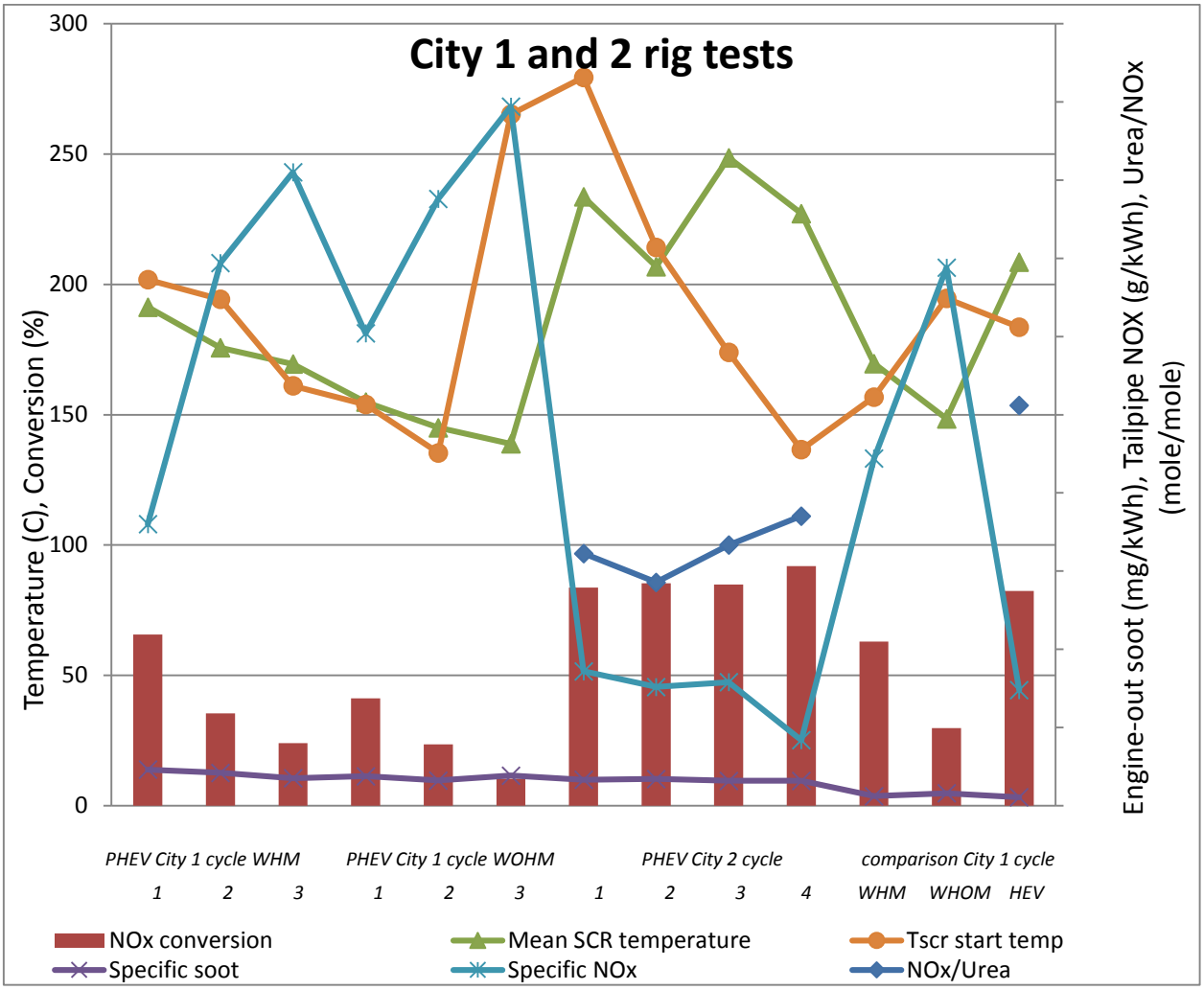

Figure 8: City 1 and City 2 rig tests for PHEV and HEV

As seen from the figure, the same tests are repeated for City 1 WHM three times, WOHM three times and City 2 tests four times. It is worth to mention that the repeated tests for each type are performed consecutively with no stop time in between. The measured engine out soot data for all cycles is in the range of 0.194 – 0.055 mg/kWh, i.e. all tested conditions are below the targeted Euro VI level (10 mg/kWh). This means that the 5l ICE used produce an exhaust flow with a low soot concentration. On the other hand, it is important to keep in mind that not only mass of soot is regulated but also number of particles which is presented further down in tables 10-14. The NO_X conversion, on the other hand, varies depending on the test conditions (test start temperature, pre-SCR temperature and urea dosage). One noteworthy observation in this figure is that urea is only injected for the PHEV City 2 measurements and for the HEV city 1 cycle. The reason for this is either that the low temperature never exceeds the set urea dosing temperature for this PHEV cycle or that the rig test operators disabled the urea dosing. A decline in NO_X conversion with each repeated PHEV City 1 experiment using heat modes is observed for the test with heat modes; starting at 65.6 %,

compared with 24 % converted NO_X for the last run (test 3). The same trend is observed for the tests without heat modes where the conversion is 41% for the first test and 10.4 % in the last run (test 6). It could be argued that decrease in conversion is a consequence of lower start temperature for the test which in turn influences the mean pre-SCR temperature for the cycle. However, considering the order of these replicated runs, with zero injected urea, one have to consider the amount of NH_3 stored inside the SCR catalyst as an important parameter for NO_X conversion. The conversion will decrease as the ammonia is gradually consumed by the SCR-reactions until more ammonia is injected and conditions for ammonia storage are fulfilled. When the NO_X conversion activity on the SCR catalyst decrease due to temperature decrease and NH_3 shortage, the tailpipe NO_X emission specific (g/kWh) will increase with each test since the replicated cycle will approximately produce the same amount of engine out NO_X and energy output (kWh) over the entire cycle.

The results from the PHEV City 1 cycle tests without heat modes show a similar pattern as with heat modes but the mean pre-SCR temperature is lower. The effect of this is less SCR activity leading to a lower reduction of NO_X.

The City 2 experiments run the engine on high power and produce sufficiently warm exhaust to heat up the SCR enough to allow for urea dosing. The conversion is considerably higher than for the City 1 cycle which is accomplished by having kinetically more favorable operating conditions, e.g. high temperature and reactant load. The last City 2 cycle run has high temperature and the highest urea dosage level and is also the cycle test which manages best to reduce the specific levels for NO_X.

On the last day of experiments three City 1 cycle tests were performed comparing a regular HEV with a PHEV with and without heat modes. The NO_X conversion for the HEV is higher due to high exhaust gas temperature and the ability to inject urea to the SCR-catalyst. The fuel economy is however far superior for the PHEV, especially in the absence of heat modes as can be seen in figure 9. The use of heat modes seems to improve the SCR performance giving lower tailpipe NO_X in g/kWh but the technique leads to increased fuel consumption and higher engine out NO_X since more fuel is combusted. All 13 rig tests show tailpipe carbon monoxide levels far below the Euro VI limit which indicates high activity over the DOC.

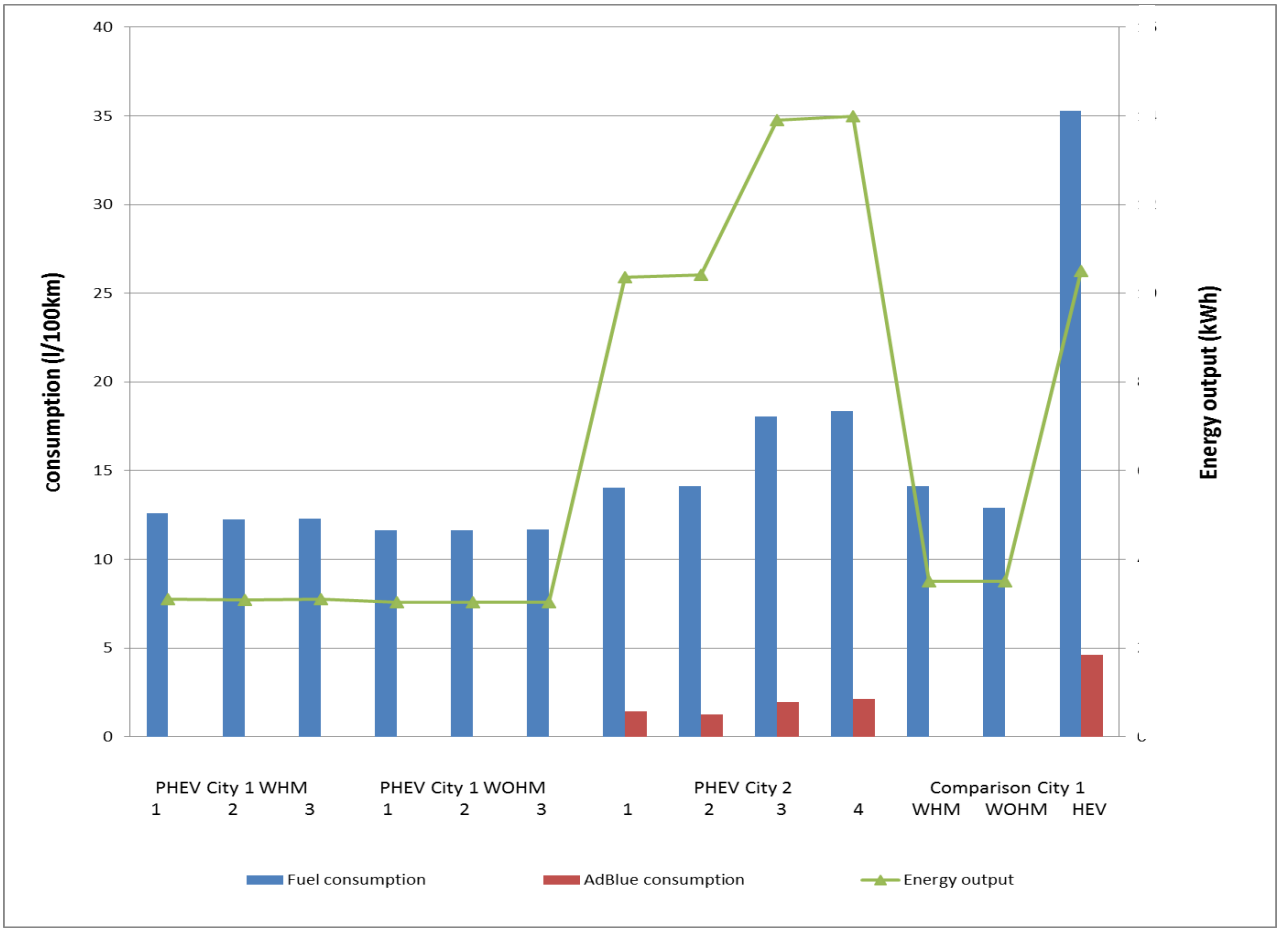

Figure9. Energy output and Fuel and AdBlue consumption for all City 1 and 2 cycle tests

It is evident from figure 9 that the PHEV City 2 cycle with high energy output and mean power has a higher fuel consumption than the PHEV City 1 cycle. One can also conclude that the addition of heat mode worsen the fuel economy, most apparently in the comparison between cycle test WHM and WOHM. This is logical since the fuel that might be injected upstream the DOC is merely used to increase the exhaust temperature and not to be utilized by the ICE to power the wheels. The high energy output for the City 2 cycle and HEV City 1 result in higher temperature in the system which allow for AdBlue injection, with a consumption of approximately one magnitude less than that of diesel fuel.

Figure 10 displays the temperature profiles for the exhaust gas upstream the SCR catalysts for City 1 cycle with and without heat modes (test 1 and test 4) and the corresponding power outputs for these two tests.

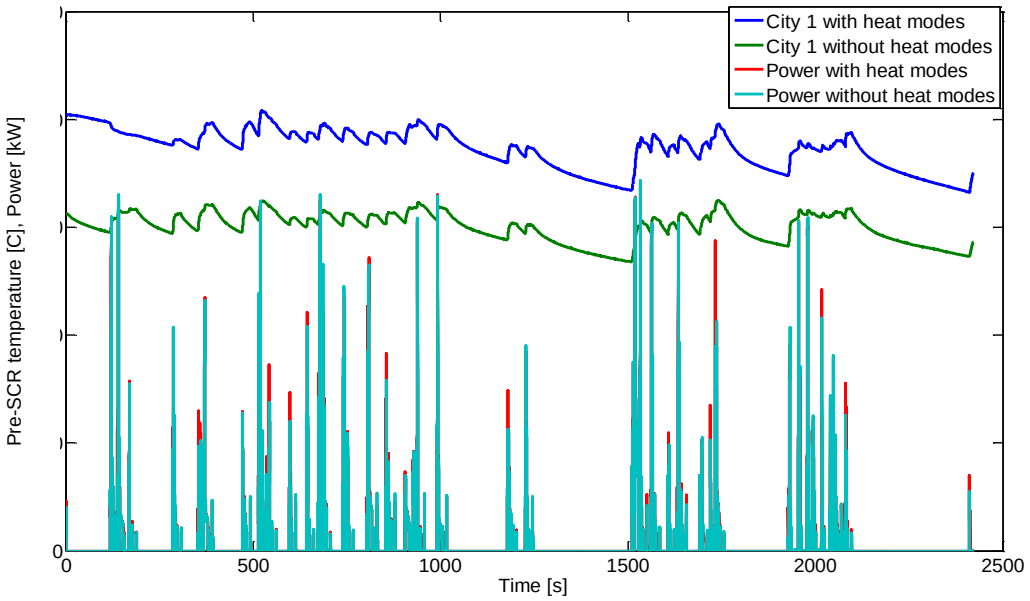

Figure10. Pre-SCR temperature for the first City 1 cycle test with and without heat modes

The shapes of the two temperature curves are similar throughout the cycle but with an approximate 40°C temperature difference (higher temperature with heat mode). In both tests, the temperatures decrease with time. However, the temperature drop for the test with heat modes is higher compared to that for the test without heat mode (35.5°C versus 19.4°C). The difference in cooling speed when the ICE engine is off might be explained by eq.A9. Assuming equal environment temperature and that the inverse of the time constant is equal in both cases, the only varying parameter is the temperature difference between SCR and environment. Since $\Delta T_{SCR\text{-}env}$ is larger for the heat mode case a more rapid temperature drop is experienced.

The time between 2097-2411 s in figure 10 is the period where the batteries are charging. The last ICE part for City 1 PHEV cycles, i.e. in the period 2411s - 2421s seen in figure 10 is not part of the cycle. Thus, this will not be included when evaluating each individual ICE period.

PHEV City 2 cycles

This section will more thoroughly investigate the PHEV City 2 cycle by looking at each ICE period for the first City 2 test. Figure 11 displays NO_X conversion (upper panel), mean SCR temperature (middle panel) and urea/NO_X molar ratios (lower panel) for all ICE periods in the first City 2 cycle test.

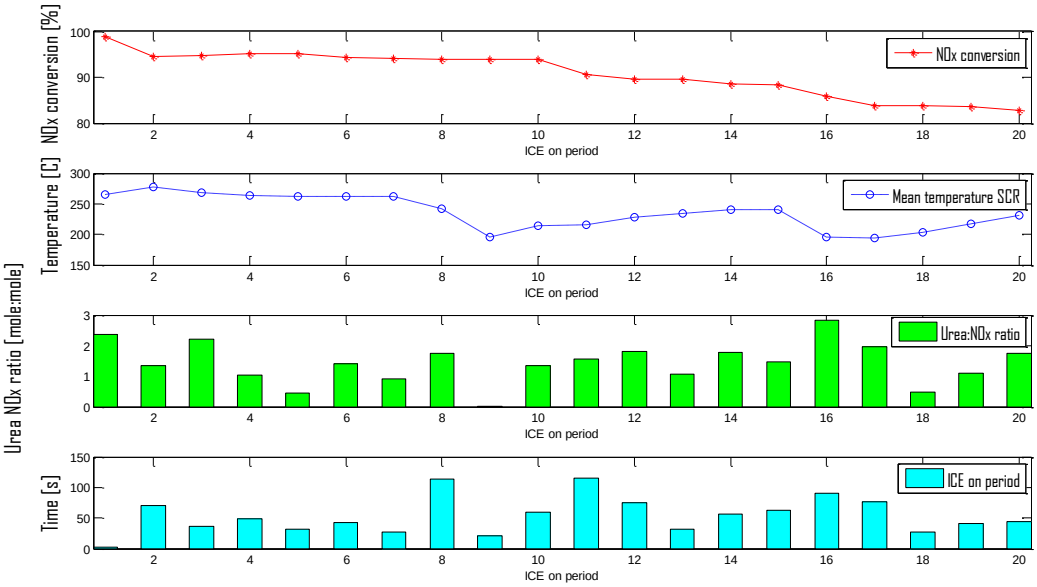

Figure11. EATS performance results from the first City 2 cycle test

During the City 2 cycle, the exhaust temperature is high enough to allow for urea dosage every time the combustion engine is working. This explains why the NO_X conversion is relatively high when the pre-SCR temperature is about 250 °C. However, as seen from the figure, NO_X conversion is slowly declining from roughly 95% to about 85% during the test time which might be a result of a decrease in average exhaust temperature upstream the SCR-catalyst during the time when the ICE is off. In addition, it is also possible that the amount of stored NH_3 is higher in the beginning of the test. The adsorbed ammonia on the catalyst reacts fast with NO_X while the process of decomposition of urea/AdBlue to NH3 might limit the SCR-reactions when, for example, the thermolysis of urea occur at temperatures below 200 °C or when the mixing of the reactants is poor, causing weak distribution over the SCR-catalyst which can result in a low NO_X conversion.

Additional data for the first test in the city 2 cycle is displayed in Figure 12. The upper panel of this figure shows the tailpipe NO_X for the ICE periods in the cycle, period start and end temperatures for each ICE period in the upper middle panel and the energy output in the lower middle panel and finally the time durations for ICE periods in the last panel.

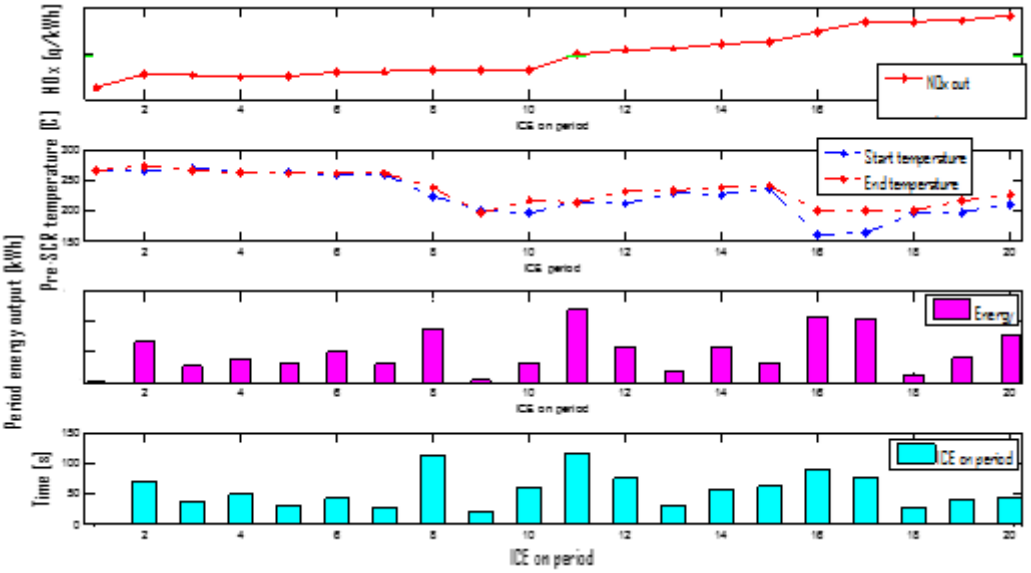

Figure12. EATS performance and engine output results from the first City 2 cycle test

As seen from the figure, the tailpipe NO_X curve is quite straight during the first 10 ICE periods while the last 10 are above and steadily increasing.

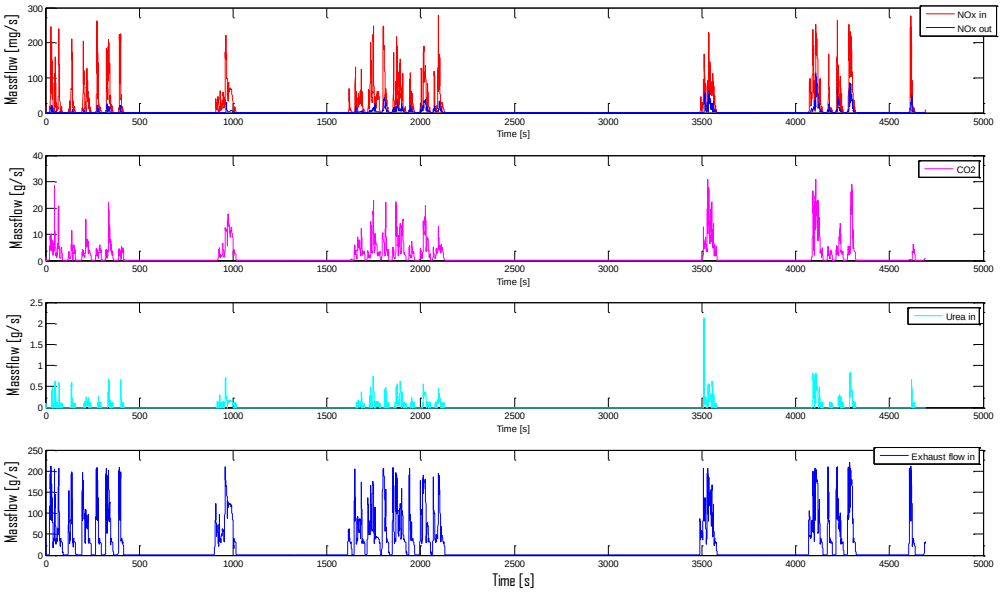

Figure13. Presenting exhaust, urea, NO_X and CO_2 mass flows

The NO_X engine-out (NO_X in) and tailpipe (NO_X out) flow data (in mg/s) in the upper panel of Figure 13 show clearly the increase in NO_X out data in relation to NO_X in data during the last five period. The Figure also show outlet CO2 flow during this test as well as the urea dosage and the total mass flow in g/s. The time intervals with zero flows correspond to conditions when the ICE is not in operation.

Figure 14 shows the power output and temperature profiles before and after the DPF as well as before the SCR. The temperature threshold for urea dosage is added in the figure for illustration. It is important here to focus the intention on the temperature profiles during the periods when the ICE is in operation. At these periods, it is clear that the pre-DPF temperature is higher than the post-DPF temperature which in turn is higher than the pre-SCR temperature. This is quite reasonable as the DPF is positioned upstream the SCR. The temperature profiles during the periods when the ICE is off (no gas flow through the EATS system) are different where the post-DPF temperature is lower than the pre-SCR temperature. This can be interpreted as the temperature drop in the SCR region is slower than that in the region between DPF and SCR probably due to less efficient insulation. A consequence of the ICE being in operation is the increase in SCR temperature as the produced exhaust passes through the EATS.

Another observation that can be made is that the DPF temperature is quite too low to enable a high passive soot regeneration activity. This means that active regeneration strategy must be taken into account and implemented.

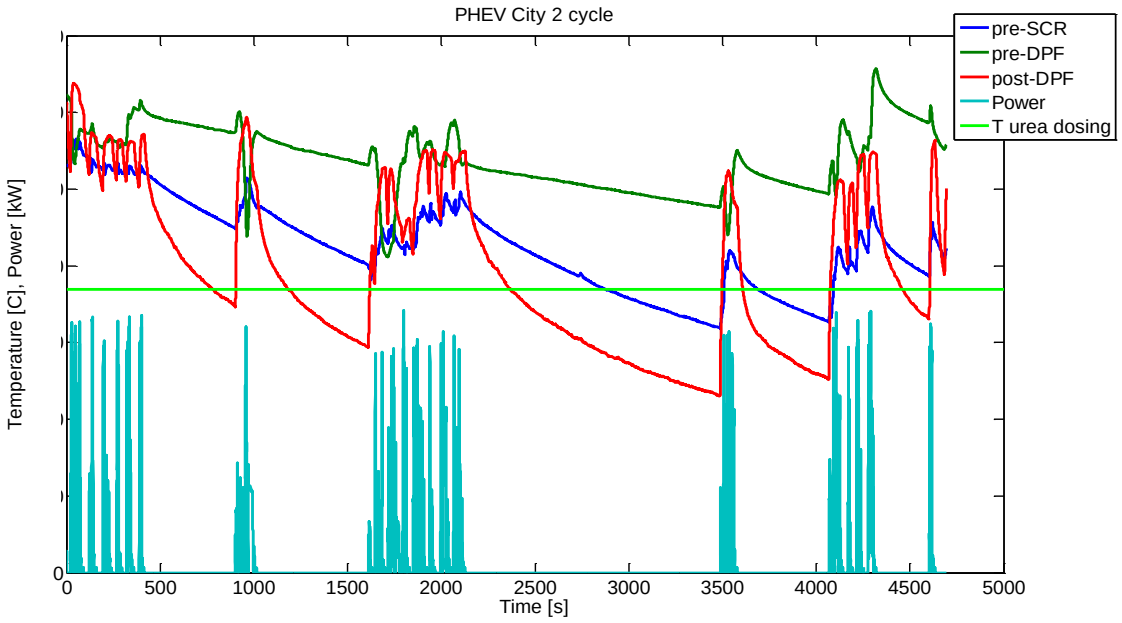

Figure14. Measured temperatures and power during the first City 2 cycle test

As was seen from Figure 8 above, the highest NO_X conversion was achieved during the fourth test of City 2 cycle where the total energy output was the highest among the PHEV cycles. The measured data for this test was analyzed to understand the reasons behind this improved NO_X conversion and these results are displayed in Figures 15 and 16.

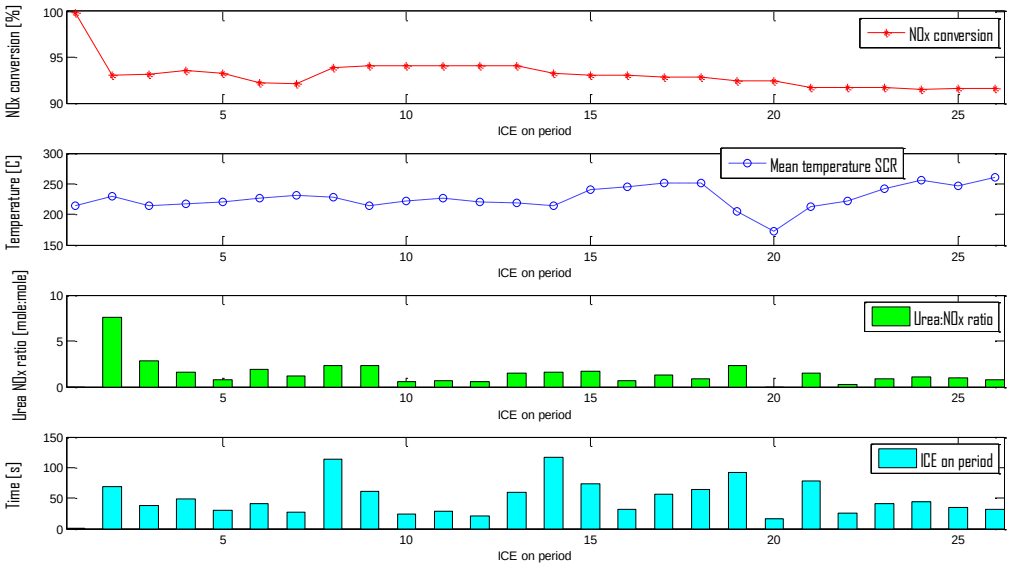

Figure 15: NO_X conversion, mean SCR temperatures, urea/NO_X ratios and step lengths during the ICE periods for the fourth test in City 2 cycle.

As seen from the upper panel in Figure 15, the NO_X conversion is above 90% during the entire test. There is a significant drop in temperature during period #20 (upper middle panel) to blow the temperature threshold for urea dosage which explain the stop in urea dosage in this period (lower middle panel). However, this period is very short (roughly 15 s) as seen from the last panel in Figure 15, thus, no significant effect is seen on NO_X conversion where probably, the stored NH3 in the catalyst is enough for the NO_X conversion activity during this period.

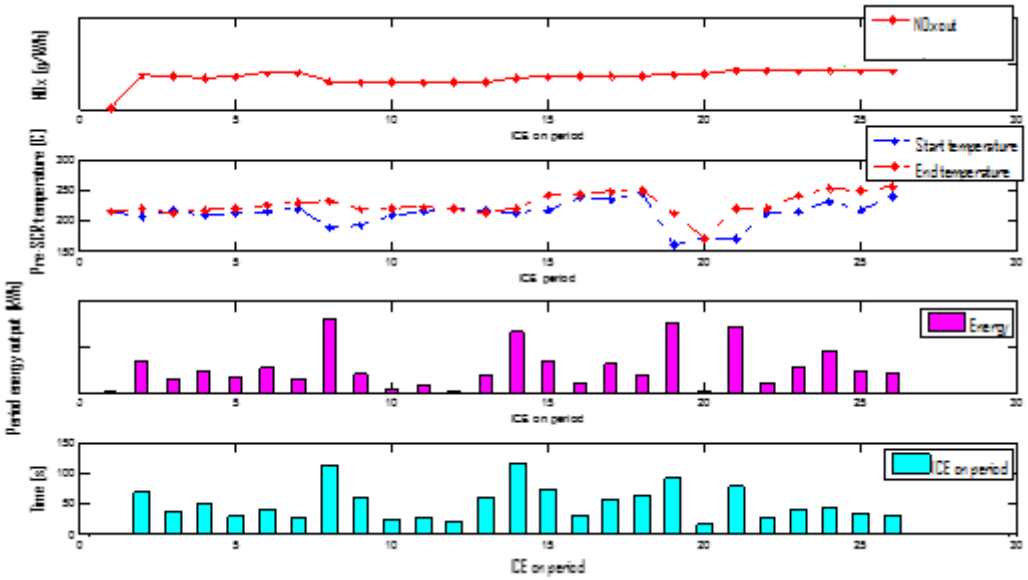

Figure16. EATS performance and tailpipe results from the fourth City 2 cycle test

A low variation in specific NO_X levels is observed throughout all 26 ICE operating periods. The test cycle seems to contain a big variation in energy output and ICE period step lengths (last two panels, respectively in Figure 16).

The total energy output or consequently the mean power output (kW) for the fourth City 2 cycle tests is as noted in figure 9 considerably higher than for the first City 2 cycle test (presented in figure 12-13) which may be a reason for the improved SCR performance. The higher power output test will produce a larger exhaust mass flow, this in combination with the higher average exhaust temperature (engine out), presented in table 10 below, result in a higher heat content for the exhaust in the last City 2 test. The increased heat supply by the exhaust gas will enhance the crucial urea decomposition, particularly by improving the thermolysis reaction which leads to a higher formation of SCR reactants, NH_3 and HCNO. A higher exhaust mass flow (higher volumetric flow) is also associated with some negative impact on the NO_X reduction due to a reduced residence time for the reactants inside the SCR-catalyst.

Table 12 displays tailpipe emission values for HC, NH_3 and also number of particles. In these tests CO out was not measured. The average HC conversion was 95.3% which gives a hint of a high CO conversion as well. The number of particles measured may be influenced by several factors such as exhaust temperature and presence of nanoparticle precursors [12]. Some common precursors are SO_3 and HC which tend to promote the formation of nanoparticles, increasing the total number of tailpipe particles and at high exhaust temperature sulfate formation are promoted. The correlation of these two influencing factors to particle number is evident as decreased exhaust temperature and HC

content seems to reduce the total particle number out. The time under $T_{urea,dosage}$ represents the percent of time when the ICE is operating and the pre-SCR temperature is below the urea dosage temperature (see figure 14), which for these PHEV City 2 cycles is around 0.5-1.4 % corresponding to 5-11 s. The surprisingly high NO_X conversion during this narrow time window might be attributed to stored ammonia on the SCR-catalyst. The last two rig tests experience a small enhancement in fuel efficiency (eq. A4) as a logical consequence of the reduction of specific fuel in g/kWh. The specific standards are normalized against the first City 2 test.

Table12. ***Tailpipe emissions and performance data from all 4 City 2 PHEV cycles, cycle time t_{cycle}=4695s. The specific standards are normalized against the first City 2 test.***

Mean exhaust in temperature (°C)	Mean pre-DPF temperature (°C)	Tailpipe specific CO_2 (%)	Tailpipe NH_3 (ppm)	Tailpipe specific HC (%)	Tailpipe specific Particles (%)	Fuel (%)	Fuel efficiency, η_f (%)	Time under $T_{urea,dosage}$ (%)	Conversion during, T< $T_{urea,dosage}$ (%)	Time ICE off (%)
251.1	270.1	-	3.17	-	-	-	31	0.89	93.4	82.9
241.4	257.9	+2	1.00	-9	-48	0	31	1.38	97.3	82.9
266.4	284.9	-5	1.14	-10	+1	-4	33	0.5	96.0	79.5
258.4	275.7	-3	0.51	-34	-52	-3.5	32	0.64	98.8	81.0

PHEV City 1 cycles with heat modes

The following section will more thoroughly investigate the PHEV City 1 cycle by looking at each ICE period for the first City 1 test with heat modes.

Figure 17 shows NO_X conversion (upper panel), mean pre-SCR temperature (upper middle panel), molar amount of tailpipe NO_X (lower middle panel) and the time duration for the periods when the ICE is in operation (last panel).

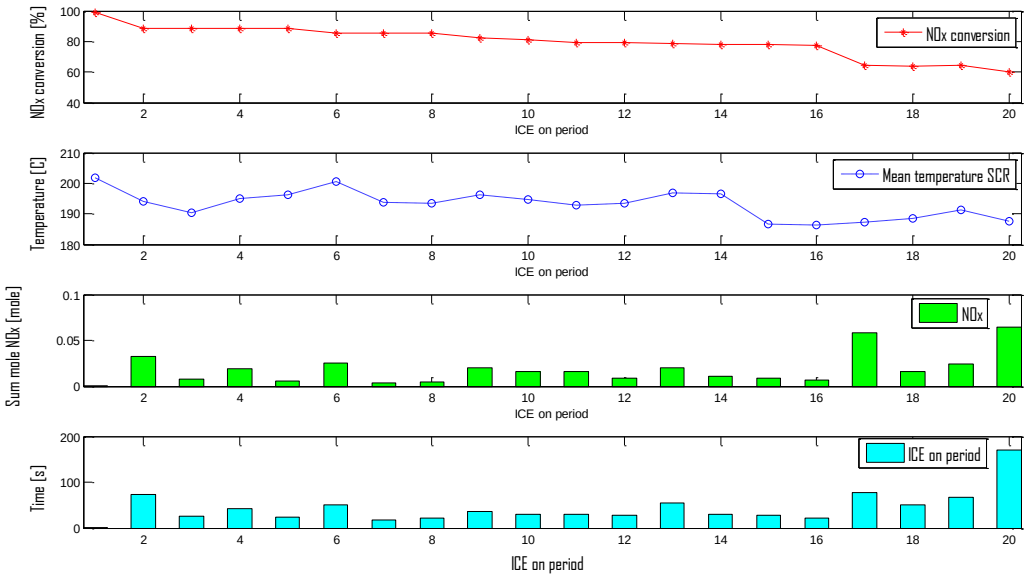

Figure17. EATS performance results from the first City 1 cycle test (with heat mode).

Additional measured data for this test (tailpipe NO_X, start and stop temperatures, the energy output and time durations for the ICE periods, are shown in Figure 18. From the test data, it was observed that no urea was injected during this test which means that the only possible source of NH_3 is stored NH_3. The first period is short leading to a negligible contribution to the overall NO_X conversion, periods 2-10 are all above 80 % NO_X conversion. The majority of the inlet NO_X comes from the latter periods. The decrease in converted NO_X is probably caused by a decline in SCR temperature and by decay in the ammonia buffer. The amount of stored NH_3 was not determined during the City 1 cycle tests, but a hypothetical amount of 16 g or 0.94 moles (see figure15) is theoretically more than enough to convert all the NO_X of 0.37 moles from this cycle test, assuming that the mole relation is 1:1 between NO_X and NH3 during the SCR reactions.

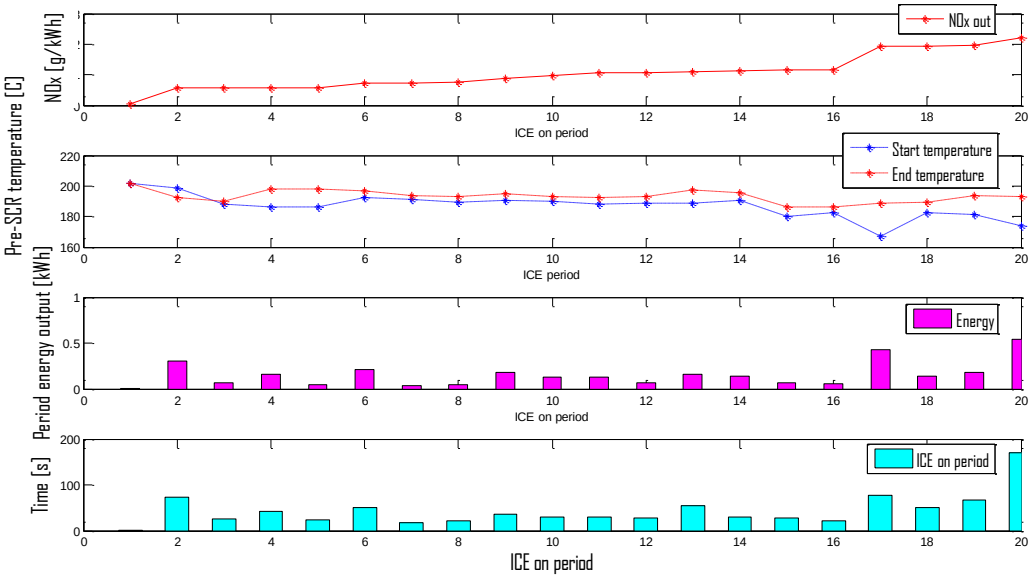

Figure18: EATS performance and tailpipe results from the first City 1 cycle test with heat modes

Figure 19 compares NO_X conversion for all three City 1 cycle with heat modes.

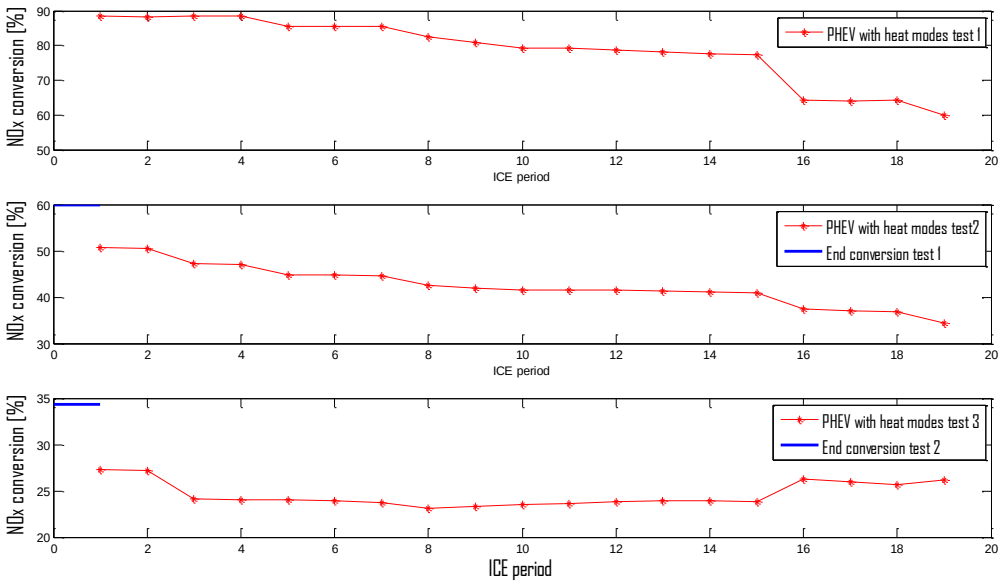

Figure19: NO_X conversion for the three consecutive PHEV City 1 cycle tests with heat modes. The first 1.3s long ICE period is removed.

This figure shows a decrease in NO_X conversion throughout all combustion periods and cycle tests, starting from approximately 90 % and ending at around 25 %. The conversion decreases since no urea is injected into the system and the stored ammonia gets consumed by the SCR reactions.

Table 13 displays mean pre-DOC and pre-DPF temperatures, tailpipe emission values and conversion for CO an HC, tailpipe particles number, fuel efficiency and percentage of time duration when the ICE is not in operation. The specific standards are normalized against the first City 1 test with heat modes.

Table13: **Tailpipe specific emission and performance data from all 3 PHEV City 1 cycles with heat modes, cycle time t_{cycle}=2421 s. The specific standards are normalized against the first City 1 test with heat modes.**

Mean pre-DOC temperature (°C)	Mean pre-DPF temperature (°C)	Tailpipe specific CO_2 (%)	Tailpipe specific CO (%)	Tailpipe specific HC (%)	Tailpipe specific Particles (%)	CO conversion (%)	HC conversion (%)	Fuel efficiency, η_f (%)	Time ICE off (%)
193.0	218.8	0	0	0	0	99.6	99.1	26	73.2
186.0	204.4	+0.2	+75	-27	-29	99.3	99.3	27	78.9
185.3	203.9	0	+216	-20	-34	98.5	99.3	27	79.0

No urea was dosed throughout these cycle tests and therefore no tailpipe NH_3 was detected. Both CO and HC conversion was high over the DOC, even with modest pre-DOC temperature. The hydrocarbon emissions out of the EATS were however too high most likely due to the inlet HC concentration which averaged 460 ppm compared to 30 ppm for the City 2 cycles. The increase in specific CO_2 emissions compared to the results presented in table 12 is caused by increased fuel consumption per kWh (consequently lower η_f) since the combustion of diesel fuel produce CO_2. The amount of particles leaving the EATS per cycle seems to follow the same behavior as for the previous table 12, were a lowering of HC content and DOC temperature decrease the particle number.

PHEV City 1 cycles without heat modes

This section focus on the results from the three City 1 cycle tests which were performed without heat modes. Figure 20 shows NO_X conversion (upper panel), mean Pre-SCR temperature (upper middle panel), engine-out NO_X (lower middle panel) and time duration for the individual ICE periods during this test (last panel).

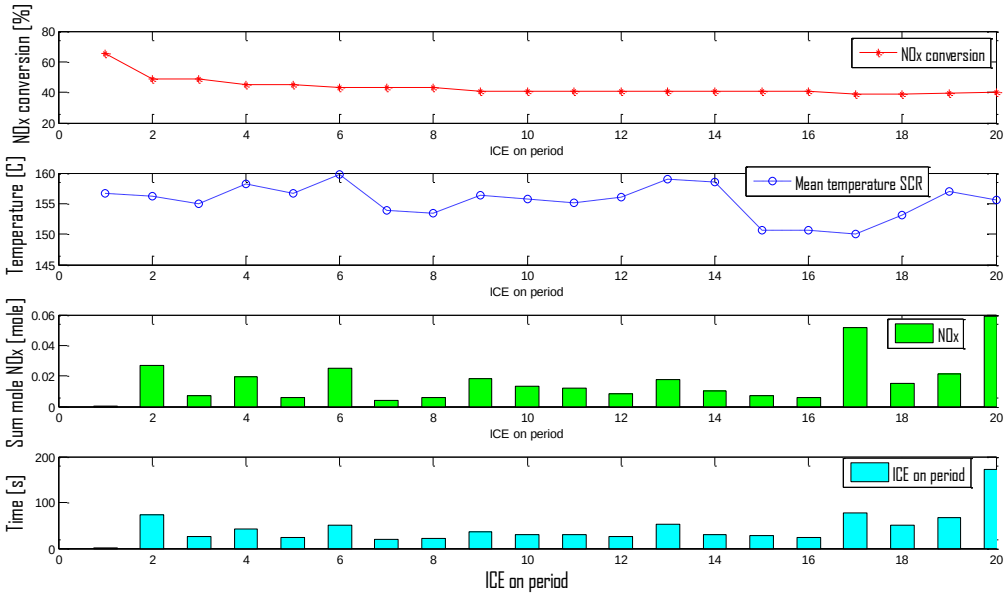

Figure 20. EATS performance results from the first City 1 cycle test without heat modes

As seen from Figure 20, the mean SCR temperature is very low (between 150 – 155 °C) in the absence of heat modes leading to low NO_X conversion activity over the SCR. As for the City 1 with heat modes the conversion decline over time, possibly due to the consumption of stored NH_3. For more information about tailpipe NO_X, ICE periods SCR- start and end temperatures, energy output and time durations, see Figure 21.

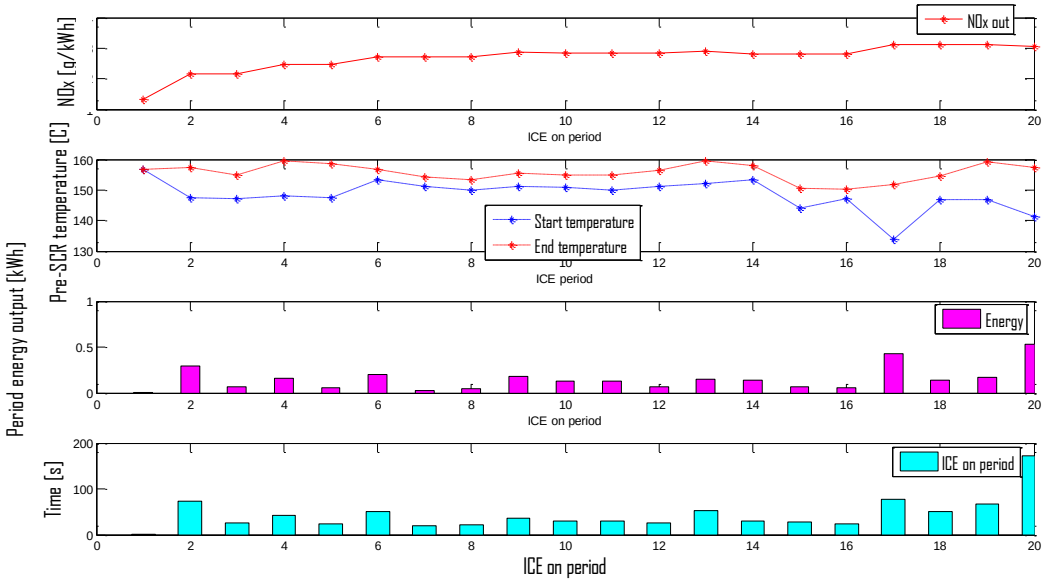

Figure21: EATS performance and tailpipe results from the first City 1 cycle test without heat modes.

The tailpipe NO_X values for the ICE periods in this test (test 1, City 1 cycle with no heat modes) are significantly higher than for the tests performed with heat modes as a consequence of less reduction of NO_X. The influence of the exhaust temperature (or SCR temperature) on the amount of tailpipe NO_X becomes evident as the temperature difference is substantial between the two cases. The amount of stored ammonia at the start of the first City 1 test with heat modes and at the start of the first test without heat modes is assumed to be equal.

An overview of the NO_X conversion during the ICE periods for all three City I cycle tests without heat modes is found in Figure 22

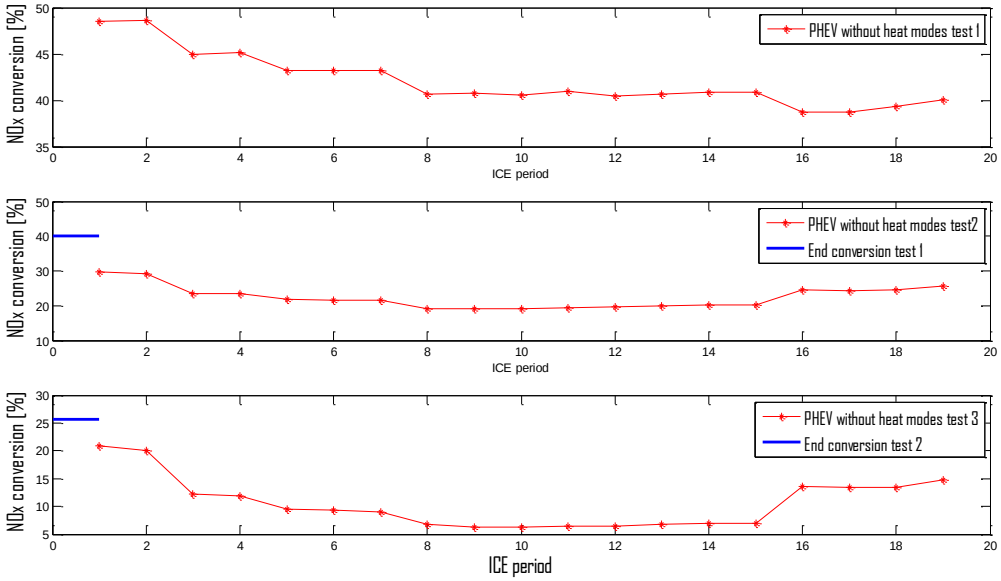

Figure22: NO_X conversion for the three consecutive PHEV City 1 cycle tests without heat modes.

Table 14 displays mean pre-DOC and pre-DPF temperatures, tailpipe emission values and conversion for CO an HC, tailpipe particles number, fuel efficiency and percentage of time duration when the ICE is not in operation.

Table14. ***Tailpipe specific emission and performance data from all 3 PHEV City 1 cycles without heat modes, cycle time t_{cycle}=2421 s***

Mean pre-DOC temperature (°C)	Mean pre-DPF temperature (°C)	Tailpipe specific CO_2 (%)	Tailpipe specific CO (%)	Tailpipe specific HC (%)	Tailpipe specific Particles (%)	CO conversion (%)	HC conversion (%)	Fuel efficiency, η_f (%)	Time ICE off (%)
166.3	178.5	-4.7	+566	-41	-43.1	96.3	97.4	27	78.5
160.9	169.3	-4.3	+1233	-34	-44.1	93.1	97.1	27	78.6
159.4	167.3	-3.1	+1983	-16	-44.1	90.8	97.1	27	78.6

The conversion of CO and HC seem to decline with lower DOC temperature as with the other preceding cycle tests (table 13), which effects the specific CO tailpipe values poorly. The CO_2 levels are a bit lower than for the PHEV City 1 cycles with heat modes. The excess CO_2 in the corresponding tests with heat modes might originate from fuel oxidation over the DOC for heat generation. The

absence of heat modes leads to a lowering of the specific tailpipe HC content since no diesel is injected by the AHI prior to the DOC.

PHEV and HEV comparison on City 1 cycle

The following section will more thoroughly investigate the HEV City 1 cycle by looking at each ICE period and compare the results with the PHEV City 1.

Figure 23 shows NO_X conversion (upper panel), mean pre-SCR temperature (upper middle panel), urea/NO_X ratio (lower middle ratio) and time duration (last panel) for all ICE periods during HEV City 1 test cycle. As seen from the figure, NO_X conversion during the first two periods is about 80%. Thereafter, it declines to below 60%, but increases gradually to about 80%.

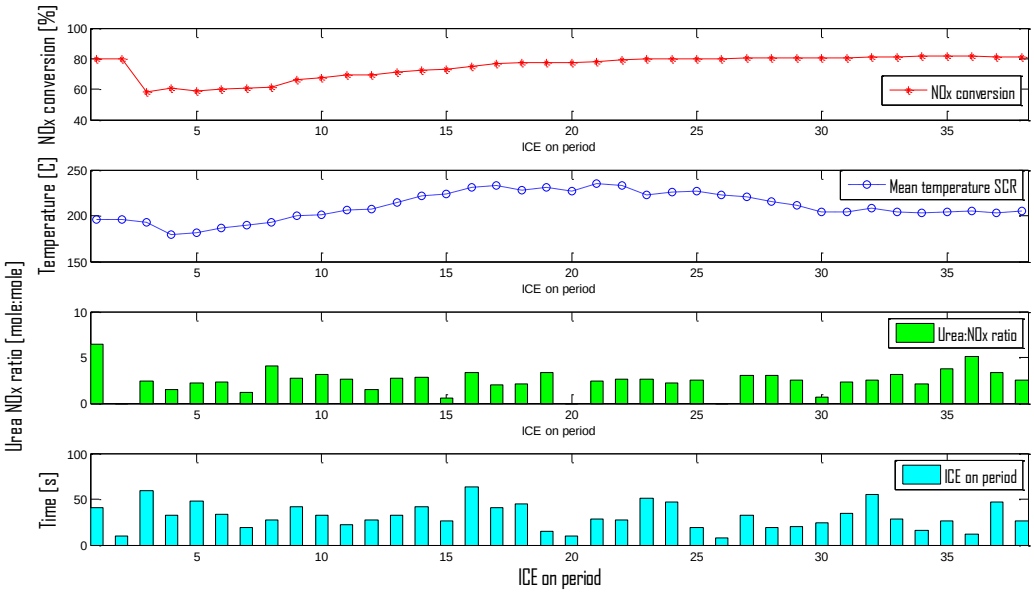

Figure23: NOx conversion, mean SCR temperatures, urea/NOx ratios and time durations for ICE periods in the HEV City 1 cycle test.

The time duration and frequency of ICE operation is approximately double for the HEV compared to the PHEV on the City cycle. In contrast to the PHEV City 1 cycle the conversion increase along the cycle with the increasing temperature after the drop in period 3. After period 25, there is a slight decline in temperature. However, NO_X conversion is not affected as the temperature is still above the kinetic limitation level and urea is still available.

Figure 24 presents tailpipe NO_X (upper panel), start and end temperatures for the ICE periods (upper middle panel), energy output (lower middle panel) and time durations for the ICE periods (last panel) for the HEV city 1 test cycle. The temperature profile seems more stable for the HEV cycle (figures 26 and 12) compared to the somewhat fluctuating SCR temperature during the PHEV cycles. The SCR is operating in a kinetically more favorable temperature region, allowing more urea to decompose and thereby promoting the reduction reactions of NO_X. The temperature starts to slowly drop after around ICE period 25, the conversion curve however continues to increase but with a smaller gradient. The overall high urea dosage might have built up ammonia in the SCR and a low NH_3 desorption rate can be expected since the average SCR temperature during ICE off is 207°C. This readily available ammonia in the catalyst will react fast with NO_X as the combustion engine is in operating mode again and the exhaust flow passes through the SCR. A possible drawback of having such a high urea/NO_X is the negative effects on the ASC.

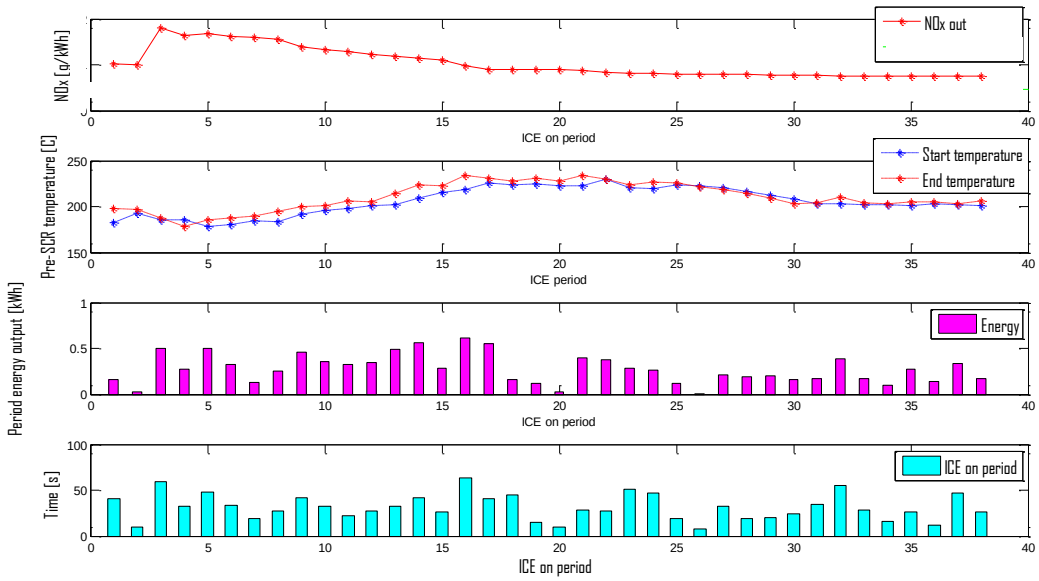

Figure 24 EATS performance and tailpipe results from the HEV City 1 cycle test

In contrast to the PHEV City 1 cycle tests the tailpipe NO_X levels decrease with each ICE period. The temperature difference is small within the ICE operating periods as can be seen in the upper middle panel where the start and end pre-SCR temperature is presented. The cooling off time between each ICE operating period is reduced compared to the PHEV tests as the number and duration of engine periods increased.

Table 15 compares mean pre-DOC and pre-DPF temperatures, tailpipe emission values and conversion for CO an HC, tailpipe particles number, fuel efficiency and percentage of time duration when the ICE is not in operation for City 1 cycle tests for HEV and PHEV with and without heat modes. The specific standards are normalized against the first City 1 test with heat modes.

Table15: ***Tailpipe specific emission and performance data from the "comparison cycle tests" with 1 PHEV City 1cycle with and without heat modes and 1 HEV city 1 cycle, t_{cycle}=2421 s, t_{HEV}=2111 s***

Type of City 1 cycle test	Mean pre-DOC temp. (°C)	Mean pre-DPF temp. (°C)	Tailpipe specific CO_2 (%)	Tailpipe specific CO (%)	Tailpipe specific HC (%)	Tailpipe specific Particles (%)	CO conversion (%)	HC conversion (%)	Fuel efficiency, η_f (%)	Time ICE off (%)
PHEV with heat modes	185.3	193.5	+6.8	-50	-36.4	-36	99.6	93.7	26	68.2
PHEV without heat modes	168.8	172.0	-3.2	+108	-29.5	-29	98.4	94.2	29	73.8
HEV	224.3	237.0	-33	-33.3	-86.2	-82	-	98.0	32	55.3

The PHEV city 1 cycle tests (1 -6 in Figure 8) differ slightly from those in Table 15 (tests 11 &12 in Figure 8) as can be seen from the percentage of time the ICE is working and energy output (figure 9). These tests are not consecutive with the other PHEV city 1 tests it is therefore difficult to determine the influence of the relative amount of stored NH_3. As seen from Table 15, the exhaust temperature for the HEV is higher than that for PHEV. This is most likely a consequence of higher engine load and longer operating duration of the engine more. The EATS performance for the HEV in this cycle test is therefore superior to that of the PHEV.

The addition of heat modes result in an increased exhaust temperature allowing for more suitable operating conditions upstream the DOC, giving reduced amounts of CO and HC. The number of particles is also substantially decreased, most likely due to the low levels of HC. By comparing the specific standard values from table 13-15 it is evident that the overall EATS performance for the PHEV on the City 1 cycle is improved when the engine operates more frequently.

6. Summary and conclusions

In this thesis raw data gathered from both on-road and rig tests have been analyzed and evaluated. The cycle tests have been performed on several bus routes to insure that the vehicle is emission compliant under different operating conditions. The rig tests being executed emulate the engine operating pattern from the actual on-road cycle test in order to estimate engine and EATS performance, e.g., tailpipe emissions, fuel and AdBlue consumption.

A regular hybrid bus and a conventional diesel bus was tested on-road, on the CBR85 cycle (City 2) during winter and summer. The prevailing EU standard was Euro V at the time and the results from the hybrid bus gave indications of an inadequate EATS, having specific tailpipe NO_X levels exceeding the measured levels for the reference bus during both winter and summer. A difference in EATS operating conditions were observed where the conventional bus had a higher temperature upstream the SCR-catalyst as well as a larger urea/NO_X ratio, these two factors is likely beneficially influencing the SCR-catalyst performance.

These tests also showed that by employing a hybrid bus on this route fuel and AdBlue consumption savings could be made up to 36% and 67% respectively. The influence of driving patterns was also evaluated by looking at data from urban and suburban parts of the cycle. It was evident for both vehicles that the fuel and AdBlue consumption were higher for the low speed urban parts, but the difference were substantially greater for the conventional bus with 30 % higher fuel consumption on the urban part compared to the suburban the corresponding value for the hybrid bus was 9 %. The reason for the modest difference with the hybrid is the electric motor, which favorable is in operation during highly fuel consuming operating conditions.

The second and last presented on-road series were performed with a PHEV named Hyperbus which include a Euro V exhaust aftertreatment system. Since the urea dosing system failed to operate, tailpipe NO_X values couldn't be determined. The specific engine out levels could however be determined and the levels for NO_X, CO and CO_2 were relatively low. The fuel consumption was only 10 l/100km.

The rig tests performed on the City 1 and City 2 cycles with a PHEV and a regular hybrid were the most thoroughly analyzed test series as these vehicles use the recent EATS and ICE of Euro VI type. The rig tests performed on the City 1 and City 2 cycles with a PHEV and a regular hybrid were the most thoroughly analyzed test series as these vehicles use the recent EATS and ICE of Euro VI type. It was presented in the result section for these tests that the tailpipe levels for PM were below the

Euro VI standard for all runs on both cycles. A decreased PN level was seen for the tests with lower pre-DOC temperature and HC amount. The addition of heat modes had a beneficial effect on the tailpipe CO levels due to an increased temperature upstream the DOC. The PHEV City 1 tests were executed with and without heat modes, the test without heat modes had an average pre-DOC temperature around 160 °C compared to 190 °C for the test series using heat modes. The higher temperature favors the HC oxidation over the DOC, however the added amount of AHI injected diesel might have been too high as an increase of specific tailpipe HC was observed during the City 1 PHEV tests.

The most challenging task for the EATS is deemed to be the reduction of NO_X, a statement which can be supported by the City 1 and 2 test series where NO_X conversion was shown to be poor on the low energy output cycle, City 1. The EATS and more notably the SCR performance is superior during the City 2 cycle tests where NO_X conversion is around 85 % for the first 3 tests and 91 % for the last. The first 2 and the last 2 PHEV City 2 tests have a difference in total energy output of around 30 %, caused by a more intensive operation of the ICE (higher mean power output). This resulted in a higher exhaust mass flow and temperature as well as a larger urea/NO_X ratio. The tailpipe NO_X levels were the lowest for the last PHEV City 2 test most likely due to the increased heat flow and urea/NO_X ratio.

During the PHEV City 1 tests no urea was injected, either since the dosing temperature was not exceeded or because the rig test operators choose to not inject urea. The data gave rise to study the influence of the pre-SCR temperature on NO_X conversion when NH_3 is stored on the catalyst. The tests with heat modes which were performed consecutively had a higher temperature than the consecutive tests without heat modes. The overall conversion and consequently tailpipe NO_X levels for the tests with heat modes were superior over the tests without heat modes, indicating that the pre-SCR temperature is a relevant factor under these conditions when the temperature is relatively low.

The average fuel consumption for the PHEV City 1 and 2 tests were 15 l/100 km, the lowest being the City 1 tests without heat mode with 12 l/100 km and the highest the last two City 2 tests where the consumption were 17.5 l/100 km.

A reduced fuel and AdBlue consumption with the degree of hybridization have been observed throughout the evaluation. Important factors have been concluded as the urea/NO_X ratio, pre-SCR temperature and exhaust mass flow. A way of achieving more favorable operating conditions for the EATS is to operate the ICE more frequently and at a higher load. The obvious drawback of this is the higher operating cost caused by the increased fuel and AdBlue consumption. It could be concluded

that the high engine load PHEV test on the City 2 cycle successfully reached specific NO_X levels while still consuming half the amount of diesel than the Euro V regular hybrid on the same cycle.

The amount of heat available upstream the SCR will determine how successful the decomposition of urea will be, which seems to be a crucial step in having a sufficient NO_X reduction.

7. Recommendations for future studies

Since the SCR have shown high activity for NO_X reduction for these tests during even relatively low temperatures and a critical step in the SCR performance is thought to be the decomposition of urea an interesting study might be to conduct experiments to find an optimal temperature region for the decomposition reactions. It would also be interesting to test alternative ammonia precursors like Amminex in order to find EATS solutions possible to be emission compliant during low ICE load. A way of preserving the heat in the system during the periods when the ICE is not in operation would also be of interest.

In order to better understand the SCR-catalyst performance behaviour for PHEVs a number of tests could be performed using an experiment series based on design of experiments principals. The input parameters could be the frequency of the combustion engine being used, the total power output by the ICE and type of test cycle. The output parameters could be tailpipe NO_X, PM and fuel consumption. The goal would be to find optimal ICE operating conditions, i.e. the engine settings giving the lowest fuel consumption while still meeting specific Euro VI levels.

8. Reference

1. Arcoumanis, C., et al., *Effect of EGR on Spray Development, Combustion and Emissions in a 1.9L Direct-Injection Diesel Engine.* SAE Technical Paper 952356, 1995.
2. Haoran Hu, Rudy Smaling, and S.J. Baseley, *Advanced Hybrid Powertrains for Commercial Vehicles*. Vol. R-369. 2014: SAE International.
3. Smith, D.E., H. Lohse-Busch, and D.K. Irick, *A Preliminary Investigation into the Mitigation of Plug-in Hybrid Electric Vehicle Tailpipe Emissions Through Supervisory Control Methods Part 1: Analytical Development of Energy Management Strategies.* SAE International, 2010. **2010-01-1266**.
4. Wang, L., et al., *Study on Thermal Management System for SCR on*

Hybrid Electric Buses. IEEE, 2011. **978-1-4244-6255-1**.
5. Lee, C.-Y.e.a., *Analysis of a Cost Effective Air Hybrid Concept.* SAE Technical Paper, 2009. **2009-01-1111**.
6. EPA. *Hydraulic Hybrid Research*

February 23, 2014.]; Available from: http://www.epa.gov/oms/technology/.
7. Heywood, J.B., *Internal Combustion Engine Fundamentals*1988: McGraw-Hill International Editions. 930.
8. JB, H., *Internal combustion engine fundamentals*1988, London: McGraw-Hill.
9. Eismark, J., *On soot oxidation in heavy duty diesel engine combustion*, 2012, Chalmers University of Technology.
10. Dieselnet, *Engine design for low emission*.
11. Johnson, T.V., *Vehicular Emissions in Review.* SAE International, 2012. **2012-01-0368**.
12. Dieselnet.
13. McAdams, W.H., *Method Of Controlling Recycling Of Exhaust Gas In Internal Combustion Engines*, 1933.
14. Campbell, L.F., *Closed Cycle Engine*, 1956.
15. Mühlberg, E., *Recycled Exhaust Gas Regulation*, 1964.
16. Nam, K., et al., *Improvement of Fuel Economy and Transient Control in a Passenger Diesel Engine Using LP(Low Pressure)-EGR.* SAE Technical Paper 2011-01-0400, 2011.
17. Russella, A. and W.S.E. a. *Diesel Oxidation Catalysts*. 2011.
18. Bowker, M., *The basis and applications of heterogeneous catalysis*1998: oxford science publications.
19. Hutzinger, O., *The Handbook of Environmental Chemistry*. Vol. 26.
20. Dieselnet, *Diesel oxidation Catalyst*.
21. Boulter, P.G., J. Borken-Kleefeld, and L. Ntziachristos, *The handbook of environmental chemistry* M. Viana, Editor 2013, Springer. p. 31 - 54.
22. Dieselnet.
23. s., B., et al., catal. Rev. Sci. Eng., 2008. **50**: p. 492-531.
24. Gekas, I., et al., *Urea-SCR Caalyst System Selection for Fuel and PM Optimised Engines and a Demonstration of a Novel Urea Injection System.* SAE Technical Paper, 2002(2002-01-0289).
25. Gieshoff, J., et al., *Advanced Urea SCR Catalysts for Automotive Applications.* SAE Technical Paper, 2001(2001-01-0514).
26. Gieshoff, J., et al., , *Improved SCR Systems for Heavy Duty Applications.* SAE Technical Paper, 2000(2000-01-0189).
27. Hammerle, R., *Urea SCR and DPF System for Diesel Sport Utility Vehicle Meeting Tier II Bin 5*, in *9th Diesel Engine Emissions Reduction Conference (DEER)*2003, Newport, RI.

28. Hirata, K., et al., *Development of Urea-SCR System for a Heavy-Duty Commercial Vehicles*, in *SAE Technical Paper*2005.
29. Hofmann, L., et al., *Onboard Emissions Monitoring on a HD Truck With An SCR System Using NOx Sensors.* SAE Technical Paper, 2004(2004-01-1290).
30. Koebel, M., G. Madia, and M. Elsener, *Selective catalytic reduction of NO and NO2 at low temperatures.* Catalysis Today, 2002. **73**(3/4): p. 239-247.
31. Cho, S.M., *Properly Apply Selective Catalytic Reduction for NOx Removal.* Chem. Eng. Prog., 1994: p. 39-45.
32. Cooper, B.J., et al., *The Development and On-Road Performance and Durability of the Four-Way Emission Control SCRT System*, in *US DOE, 9th Diesel Engine Emissions Reduction Conference (DEER)*2003, Newport.
33. Song, G. and G. Zhu, *Model-Based Closed-Loop Control of Urea SCR Exhaust Aftertreatment System for Diesel Engine.* SAE Technical Paper, 2002(2002-01-0287).
34. Kato, N., H. Kurachi and Y. Hamada, *Thick Film ZrO2 NOx Sensor for the Measurement of Low NOx Concentration.* SAE Technical Paper, 1998(980170).
35. Sluder, C.S., et al., *Low Temperature Urea Decomposition and SCR Performance.* SAE Technical Paper 2005-01-1858, 2005.
36. Sappok, A. and V. Wong, *Ash Effects on Diesel Particulate Filter Pressure Drop Sensitivity to Soot and Implications for Regeneration Frequency and DPF Control.* SAE Technical Paper, 2010(2010-01-0811).

Appendices

Appendix 1. Equations used

- $\Delta Q = \Delta m * C_P * (T_{Combustion} - T_{EGR})$ (A1)

Where Δm represents the added EGR mass flow and C_P is the denotation for the average specific heat capacity.

The power P in kW delivered by the internal combustion engine (ICE) and absorbed by the dynamometer is the product of torque and angular speed:

- $P = 2\pi NT \times 10^{-3}$ (A2)

Where N is the angular speed in rev/s and T is the torque expressed in Nm.

The total energy output over the cycle E_{cycle} is expressed in kWh and is calculated in the following way:

- $E_{cycle} = \frac{\sum_{cycle\ start}^{cycle\ end} P(kW)}{3600 \times s} \times h$ (A3)

The specific fuel consumption, sfc, which measure how effective the ICE use the fuel supplied to produce energy:

- $sfc = \frac{m_{f,cycle}}{E_{cycle}}$ (A4)

The specific fuel consumption unit is in g/kWh and $m_{f,cycle}$ is the total mass of fuel during the entire cycle in grams.

The fuel conversion efficiency η_f is expressed as:

- $\eta_f = \frac{3600}{sfc \times Q_{HV}}$ (A5)

Where Q_{HV} with unit MJ/kg is the higher limit heating value of the fuel, for diesel it is assumed to be 43 MJ/kg during these tests. The unit for sfc in these calculations is in g/kWh.

The mass flow of the emissions are calculated by this expression:

- $\dot{m}_{i,j} = \frac{m_{exhaust} \times n_{i,j} \times M_i}{M_{exhaust} \times 10^6}$ (A6)

Where the unit for the emissions and exhaust mass flow is in g/s, $M_{i,j}$ is the denotation for molecular mass (g/mole) and n the mole concentration (ppm). , The index i indicates the specie and j whether engine out or tailpipe is observed.

Specific emissions for the cycle sEmission (g/kWh) are the total mass of pollutant per unit energy output:

- $SEmission_{i,j} = \frac{m_{i,j}}{E_{cycle}}$ (A7)

Where $m_{i,j}$ is the total mass of the cycle, i indicates the pollutant (HC, CO, CO_2, PM or NO_X) and j whether engine out or tailpipe is measured.

The specific particle number sPN is determined in the following way:

- $sPN = \frac{\sum V_{exhaust} \times PN}{E_{cycle}}$ (A8)

Here $V_{exhaust}$ represents the volumetric flow (m^3/s) of the exhaust gas and PN the number of particles per cubic meter (particles/m^3). The unit for sPN is in (particles/kWh).

The cooling and temperature decrease of the SCR-catalyst may be explained by the following expression:

- $T_{SCR}(t) = T_{env} + (T_{SCR}(0) + T_{env})e^{-hAt/C}$ (A9)

Where T is temperature in kelvin, index env denotes the surrounding EATS, h the convective heat transfer coefficient (W/m^2K), A the heat transfer area of the SCR (m^2), C the SCR heat capacity (J/K) and t, the time in seconds

Appendix 2. Figures from the MD hybrid and plug-in hybrid rig tests

PHEV City 1 with heat modes

The measured engine-out and tailpipe NOx, CO2 and exhaust flow data for the first City 1 cycle test with heat modes are shown in Figure 20 (panel 1 – 3, respectively)

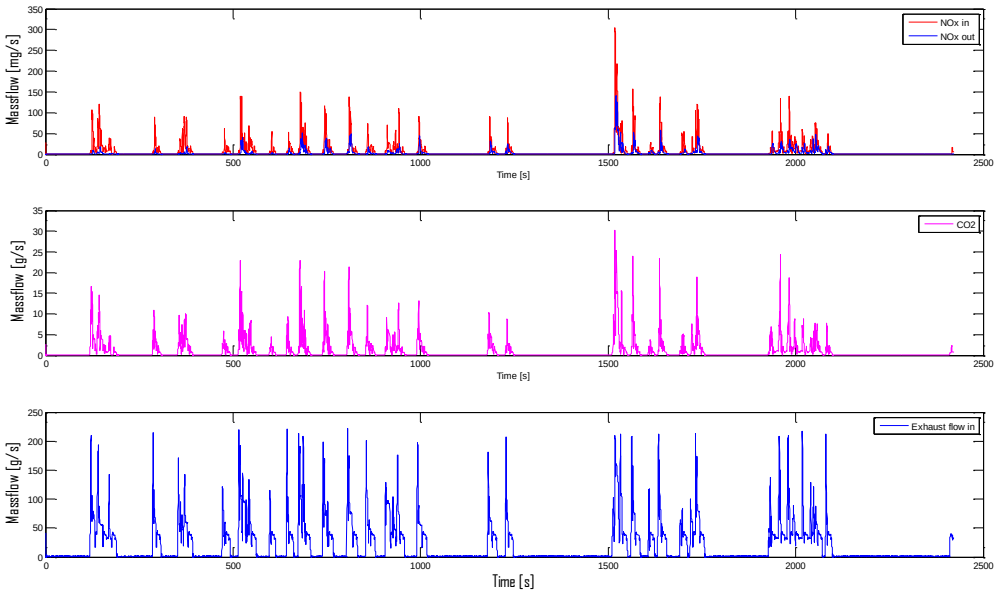

Figure20: Engine-out and tailpipe NO_X, CO_2 and exhaust mass flows for the first city 1 cycle test with heat modes.

PHEV City 1 without heat modes

Engine-out NOx and tailpipe NO_X and CO_2 mass flows for this test are presented in Figure 23.

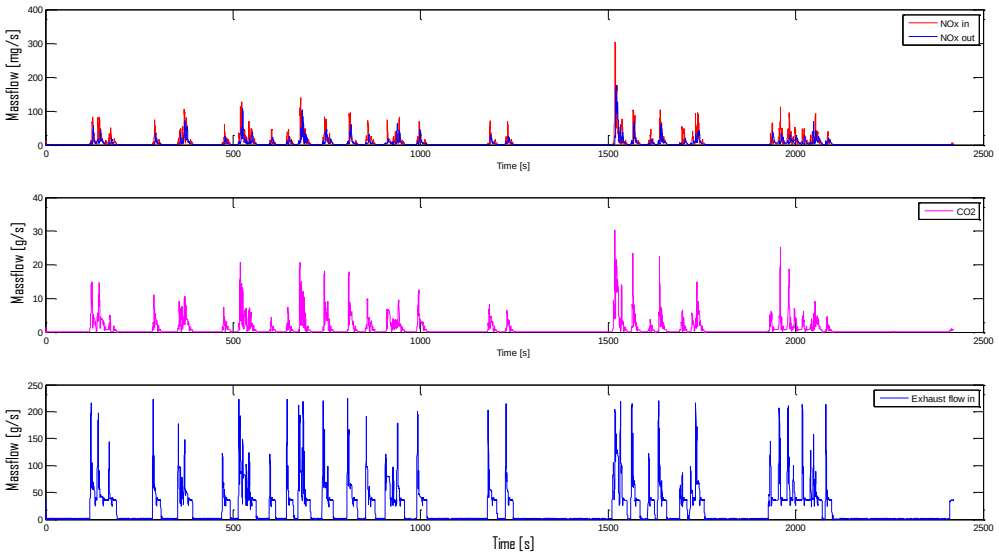

Figure23: Engine-out NOx and tailpipe NO_X and CO_2 mass flows for the first City 1 test without heat modes.

HEV City 1

Figure 27 shows the engine-out and tailpipe NOx, CO_2, NH_3 and total exhaust flows for the HEV City 1 cycle test.

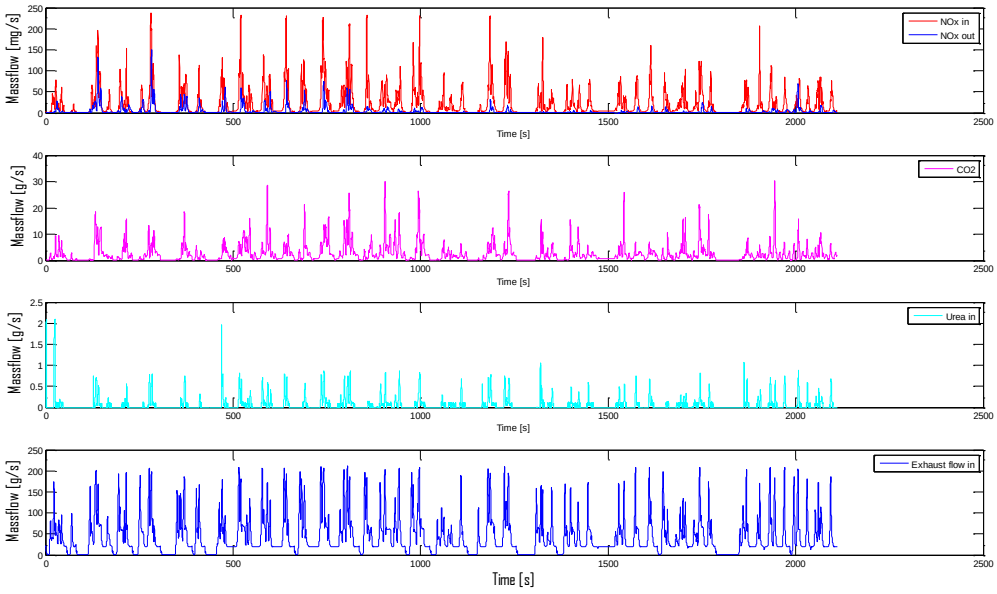

Figure27: NO_X (engine-out and tailpipe),CO_2,NH_3 and total exhaust mass flows for the HEV City 1 cycle.